NJC

Accepted Manuscript

This is an *Accepted Manuscript*, which has been through the Royal Society of Chemistry peer review process and has been accepted for publication.

Accepted Manuscripts are published online shortly after acceptance, before technical editing, formatting and proof reading. Using this free service, authors can make their results available to the community, in citable form, before we publish the edited article. We will replace this *Accepted Manuscript* with the edited and formatted *Advance Article* as soon as it is available.

You can find more information about *Accepted Manuscripts* in the Information for Authors.

Please note that technical editing may introduce minor changes to the text and/or graphics, which may alter content. The journal's standard Terms & Conditions and the Ethical guidelines still apply. In no event shall the Royal Society of Chemistry be held responsible for any errors or omissions in this *Accepted Manuscript* or any consequences arising from the use of any information it contains.

ROYAL SOCIETY OF CHEMISTRY

www.rsc.org/njc

Experimental and computational analysis of supramolecular motifs involving Csp2(aromatic)-F and CF3 group in organic flustrates

Piyush Panini[a], *Rajesh G.Gonnade*[b], *Deepak Chopra*[a]*

[a] *Crystallography and Crystal Chemistry Laboratory, Department of Chemistry, Indian Institute of Science Education and Research Bhopal, Madhya Pradesh, India-462066. Fax: 91-0755-6692370. Email: dchopra@iiserb.ac.in*

[b] *Center for Materials Charaterization (CMC), CSIR-National Chemical Laboratory, Pune-411008, India.*

Abstract:

A detailed experimental (SCXRD) and theoretical (PIXEL and QTAIM) investigation of the evolution of different supramolecular motifs formed *via* the presence of both C(sp^2)/(sp^3)-F group in the crystal packing have been performed in a series of newly synthesized substituted benzanilides (containing "*both*" the fluorine and the trifluoromethyl group in the same molecule) along with previously reported similarly related crystal structures [*CrystEngComm*, 2008, **10**, 54 – 67; *CrystEngComm*, 2012, **14**, 1972−1989, *CrystEngComm*, 2013, **15**, 3711−3733]. It was observed that the highest stabilized molecular motifs primarily consist of C(sp^2)-H···F-C(sp^2) H-bond in preference to C(sp^2)-H···F-C(sp^3) H-bond in the crystal. The motifs involving C(sp^2)-H···F-C(sp^2)/(sp^3) H bonds were observed to be present over the entire distance range between 2.2 to 2.7Å, albeit the difference in energies of stabilization involving fluorine atoms attached to sp^2 and sp^3 carbon is not significant in molecular crystals. From QTAIM analysis, the C(sp^2)/(sp^3)-F···F-C(sp^2)/(sp^3) interactions were observed to be closed shell in nature and provide *local* stabilization, indicating the formation of bond, similar to weak hydrogen bonds observed in crystals.

Introduction:

The introduction of a fluorine atom to the carbon atom (termed as "Organic Fluorine") can lead to the formation of many weak interactions like C-H···F-C hydrogen bond [**1-2**], C-F···F-C [**3-4**]

and C-F···π [**5-7**] interactions and study of these interactions involving organic fluorine is still an expanding area of research amongst the scientific community [**8**]. However, there has been an enduring discussion regarding the ability of organic fluorine to act as a hydrogen bond acceptor [**9 - 18**] because of its low polarizability. However, crystal structure analysis of fluorobenzenes [**12**] and ribonucleic acids [**13**] unfasten the area of research regarding the study of interactions involving organic fluorine. Further, such interactions with the protein active site through C–F···C=O, and C–F···H–C_α interactions have been reviewed by Diedrich *et. al.***[19].** Since then many studies *via* inputs from crystallography, spectroscopy and theoretical calculations have established the fact that the interactions involving fluorine are ubiquitous and can play an important role in the stabilization of the crystal packing and influence the phenomenon and properties in the solids state, one such example is polymorphism. The extensive literature on compounds related to the presence of organic fluorine has been excellently combined in reviews [**8**, **20-22**] and a book chapter [**23**]. It was initially postulated that the weak interactions involving fluorine like C-H···F-C hydrogen bonds are only significant in the absence of any other strong intermolecular forces [**24**]. The analysis of the nature of fluorine interactions on many molecules has been performed, wherein the possibility of the formation of strong hydrogen bonds was eliminated. Amongst these, benzene **[12**, **18]**, naphthalene, anthracene and phenanthrene **[16],** isoquinolines [**24-25**], trifluoroacetophenones [**26**], *N*-phenylmaleimides and corresponding phthalimides [**27**], benzonitriles [**28**], pyridines [**29**], azobenzenes [**30**], *N*-benzylideneanilines [**31-32**], toluene [**33**], *N*-methyl-*N*-phenylbenzamides **[34]** are a few examples to be mentioned. There is not sufficient literature on the study of these intermolecular interactions in molecules wherein strong intermolecular forces are present **[20]**. However, fluorinated *N*-(2-Chloropyridin-4-yl)-*N′*-phenylureas [**35**], fluoro-*N*-(pyridyl)benzamides [**36**], fluorine-substituted benzoic acid **[37]**, fluorine-substituted benzimidazoles [**38**] are a few examples wherein evaluation of interactions involving fluorine were realized in the presence of a strong hydrogen bond. Keeping in mind the above-mentioned points, improvements aimed towards the understanding of the nature, capability and energetics of interactions involving organic fluorine (in particular C-H···F and C-F···F-C interactions) in the presence of strong hydrogen bond has been undertaken by our research in the past last few years **[17, 39 - 41]**. Our main goal was (i) a systematic exploration of the participation of the fluorine atom in different intermolecular interactions (ii) robustness of the interaction (i.e how often they are present) in the formation of different supramolecular

motifs (iii) role of hydridization of C-atom to which fluorine is attached and finally (iv) calculation of stabilization energy and topological parameters such as the electron densities (ρ), Laplacian ($\nabla^2\rho$), local potential energy (V_b), kinetic potential energy (G_b) at the bond critical point by Quantum Theory of Atoms in Molecules (QTAIM) **[42]**. In this regard, a large library of molecules containing the organic fluorine group have been synthesized, crystallized and investigated for different intermolecular interactions involving organic fluorine. The systems were designed such that these only have one strong donor and acceptor (the amide group -NH-C=O- in our works) atom which connects at least one phenyl ring wherein the position of the fluorine (connected to C-atom) of different hybridization, [C(sp^2)-F & -C(sp^3)-F3 group] many vary, keeping the main molecular connectivity invariant. Hence, different molecules, namely fluorine substituted benzanilides **[17]**, fluorine and -CF_3 substituted *N*-phenylacetamides and *N*-methylbenzamides **[39]**, -CF_3 substituted benzanilides have been studied **[40]**. The purpose of selecting the CF_3 group was as follows: (i) The –CF_3 group being strongly electron-withdrawing in nature increase the acidity of hydrogen atoms in its vicinity (ii) better H-bond acceptor abilities of C(sp^3)-F can be exploited (iii) in addition to C-H···F-C hydrogen bonds, the propensity of formation of other interactions namely C-F···F-C and C-F···π is now increased (iv) in addition to all the above-mentioned points, a comparative study about the role of hybridization of the C-atom to which fluorine is attached can be achieved in the crystal.

Therefore, we have synthesized a library of substituted benzanilides (eighteen in number) containing both the fluorine and trifluoromethyl group on the same molecule (**Scheme 1**). Initial investigations on two molecules in this series, namely *N*-(4-fluorophenyl)-3-(trifluoromethyl) benzamide and 4-fluoro-*N*-[3-(trifluoromethyl)phenyl]benzamide, demonstrated existence of short H-bonds with organic fluorine in the presence of strong N-H···O=C H-bonds **[41]**. The nature of these interactions was tested with criteria for H-bond proposed recent by IUPAC **[43]** and has also been analyzed by the PIXEL method **[44 - 47]** and the QTAIM approach **[42]**. It is now well established that the C-H···F interactions at short distances are indeed a "true H-bond" and these are not the consequence of crystal packing. In this current work, along with the detailed crystal packing analysis of the remaining newly synthesized compound in this series, our main focus will be on the (i) identification of different robust or reoccurring motifs formed by the interactions involving organic fluorine in the crystal (ii) investigations of these in terms of their nature, energetics and topological properties by the PIXEL method and the QTAIM

approach (iii) comparative study about the role of hybridization [**48**] of the C-atom to which fluorine is attached, based on the inputs obtained from current and previous series of molecules **[17, 39 -40]** having similar molecular framework.

Experimental section:

All the compounds were synthesized by the procedure that is already reported in the literature **[40]**. **Scheme 1** describes the general route for the synthesis of all the 18 compounds and their corresponding nomenclature code used in this paper. All the synthesized compounds were characterized by FTIR [**Fig. S1(a)-(p)**], and ^{1}H NMR [**Fig. S2(a)-(p)**] (**Section S1**). Melting points were recorded with DSC [**Fig. S3(a)-(p)**] on the pure powder compounds. Powder X-ray diffraction (PXRD) data were recorded for all the solid compounds and then compared with their calculated PXRD patterns [**Fig. S4(a)-(p)**]. In order to ensure the phase purity, a profile fitting refinement (**Section S2)** was performed using JANA2000 [**49**]. In the case of 1F2T, 2F3T, 2T1F and 3T1F, high values of the profile fitting parameters (Rp, Rwp) were observed, which may indicate the possibility of the presence of more than one phase in the bulk powder.

The details on all the crystallization experiments of all the solid compounds from different solvents and solvent mixtures are presented in the ESI (**Table S1**).

Data collection, structure solution and refinement

Single crystal X-ray diffraction data were collected on Bruker AXS SMART APEX II CCD diffractometer at 100 K. All the data were collected at 100(2) K. All the crystal structures were solved by direct methods using SIR 92 **[50]** and refined by the full matrix least-squares method using SHELXL2013 **[51]** present in the program suite WinGX **[52]**. The non-hydrogen atoms were refined anisotropically and the hydrogen atoms bonded to C and N atoms were positioned geometrically and refined using a riding model with U_{iso}(H) = 1.2Ueq [C(sp^2)]. The disorder associated with the CF_3 group (in case of compounds **2F2T** and **2T1F_w**) and positional disorder of F-atom (in case of compounds **1F1T**, **2F1T**, **2F2T**, **2T1F**, **2T1F_w** and **2T2F**) were modeled with PART command in SHELXL 2013 at two independent orientations (major component was labeled 'A') (Fig. S5, ESI). Molecular and packing diagrams were generated using Mercury software **[53]**. **Table S2** lists all the crystallographic and refinement data. *ORTEP*s of all compounds were presented in **Figures S5(a) – S5(m)** in the ESI.

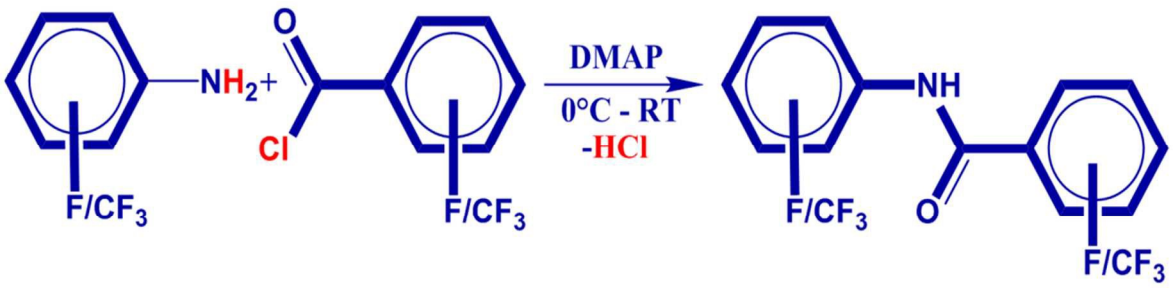

entry	A	B	Code	*entry*	A	B	Code	*entry*	A	B	Code
1	*o*-F	*o*-CF_3	**1F1T**	7	*o*-F	*p*-CF_3	**1F3T**[a]	13	*o*-CF_3	*m*-F	**1T2F**
2	*m*-F	*o*-CF_3	**2F1T**	8	*m*-F	*p*-CF_3	**2F3T**	14	*m*-CF_3	*m*-F	**2T2F**
3	*p*-F	*o*-CF_3	**3F1T**[a]	9	*p*-F	*p*-CF_3	**3F3T**	15	*p*-CF_3	*m*-F	**3T2F**[a]
4	*o*-F	*m*-CF_3	**1F2T**	10	*o*-CF_3	*o*-F	**1T1F**[a]	16	*o*-CF_3	*p*-F	**1T3F**
5	*m*-F	*m*-CF_3	**2F2T**	11	*m*-CF_3	*o*-F	**2T1F**[c]	17	*m*-CF_3	*p*-F	**2T3F**[b]
6	*p*-F	*m*-CF_3	**3F2T**[b]	12	*p*-CF_3	*o*-F	**3T1F**	18	*p*-CF_3	*p*-F	**3T3F**

[a] Single crystal suitable for SCXRD could not be obtained; [b] Reported in ref **[41]** ; [c] observed also as its hydrate (code: **2T1F_w**).

Scheme 1: Synthetic scheme for all the compounds along with their nomenclature plan used in this manuscript are presented.

Computational tools and theoretical calculations:

PIXEL method [in CLP computer program package (version 10.2.2012)] has been used for the interaction energy of the selected molecular pairs, extracted from the crystal packing and related by the corresponding symmetry element as mentioned in our previous work **[41]**. In the method, the total interaction energy is partitioned into their Coulombic (E_{coub}), polarization (E_{pol}), dispersion (E_{disp}) and repulsion (E_{rep}) contributions. In case of disordered molecules, the molecular conformation with the maximum population was considered for the calculations. PIXEL method was observed to provide better and useful insights towards the nature of different types of intermolecular interactions present in the different molecular pairs/motifs **[54 -57]**. The PIXEL interaction energy was further compared with the interaction energies obtained from theoretical calculations at DFT+Disp/B97D **[58 -59]** level at higher aug-cc-pVTZ basis set using TURBOMOLE **[60]**. The hydrogen atoms were moved to neutron values (1.083 Å for C–H) before the calculations. The basis set superposition error (BSSE) for the interaction energies was

corrected by using the counterpoise method **[61]**. **Table S3** (divided into two parts: S3a and S3b, separately for C-F···F-C in **Table S3b**) lists the selected intermolecular interactions (in the decreasing order of their stabilization energy) in different motifs along with their interaction Energies (I.E.) of the motifs. In case of highly disordered compounds **2T1F_w** [having rotational disorder associated with CF_3 group and positional disorder of the fluorine atom at the phenyl ring along with the presence of half molecule of water in the asymmetric unit, Fig. S5(h)], PIXEL calculation have not been performed. Instead, BSSE corrected interactions energies for the selected dimers were calculated at DFT+Disp/B97D level using aug-cc-pVTZ basis set (**Table S5**).

Analysis of Topological Parameters (QTAIM calculations)

Topological calculations on the selected dimers at the crystal geometry were performed with same procedure as mentioned previously **[41]** using AIMALL (version 13.05.06) **[62]**.The selected topological parameters like electron densities (ρ_c), Laplacian ($\nabla^2\rho_c$), local potential energy (V_b), and kinetic energy density (G_b) at the bond critical points (BCPs) were calculated. The dissociation energies for the different intermolecular interactions were also estimated through the following two empirical approaches: (i) D. $E^V(int) = -0.5\ V_b$ (in atomic units) **[63]** and (ii) $D.E^G(int) = 0.429\ G_b$ (in atomic units) **[64 - 65]** ; where D.E(int) is the dissociation energy of the interaction. Interaction energy (I.E) = −D.E. V_b and G_b are the local potential and kinetic energy density at the bond critical points (BCPs), respectively. The results of the topological analysis on the different molecular pairs are presented in section S4 (**Table S4 & S5)** in ESI. Topological parameters of for the selected C-H···F and C-F···F-C interactions in different motifs along with their dissociation energy is presented in **Table S4b**. Compounds having disorder associated with CF_3 group or fluorine (positional disorder) were not considered for the calculations except for **1F1T** and **2T2F** wherein the positional disorder of fluorine with occupancy ratio at the two positions were observed to be 0.875(2):0.125(2) and 0.944(3): 0.056(3) respectively. In these cases, the molecular conformation with the maximum population was considered for the calculations.

Results and Discussions:

1) *N*-(2-fluorophenyl)-2-(trifluoromethyl)benzamide (1F1T):

The compound **1F1T** crystallizes in the orthorhombic non-centrosymmetric space group $Pna2_1$ with Z = 4. A strong N-H···O=C H-bond along with a weak C-H···π hydrogen bond (motif **I**, -12.7 kcal/mol, **Table S3a**) was observed to connect the molecules along the crystallographic *a*-axis in the formation of the molecular chain [**Fig. 1 (a)**]. Such chains are interconnected *via* weak C-H···F-C_{sp3} hydrogen bond (motif V, -1.5 kcal/mol). Furthermore, there exists formation of the herringbone pattern observed down the *bc* plane in the crystal packing, stabilized via the presence of motif **II** (involving C-H···O, C-H···F-C_{sp2} hydrogen bond, -6.2 kcal/mol) and weak C-H···F-C_{sp3} hydrogen bonds in motif **IV** (-1.9 kcal/mol). Weak C-H···O=C and C-H···F-C_{sp3} hydrogen bonds were found to stabilize the crystal packing (motif III, -4.8 kcal/mol) in the generation of a molecular chain [**Fig. 1(c)**]. It is to be noted that the stabilization energy for a C-H···F hydrogen bond was reported to be ~ -0.40 kcal/mol (-1.6 kJ/mol) by *ab initio* theoretical calculation for the neutral molecule by D'Oria & Novoa **[66]**.

The presence of weak C-H···F-C hydrogen bonds in the motifs **III, IV** and **V** were characterized topologically by using the QTAIM approach. There were presence of (3, -1) bond critical points (BCPs) recognized for these interactions (**Table S4b**) along with other related interactions present in the respective motifs [**Fig. 1(d)**].

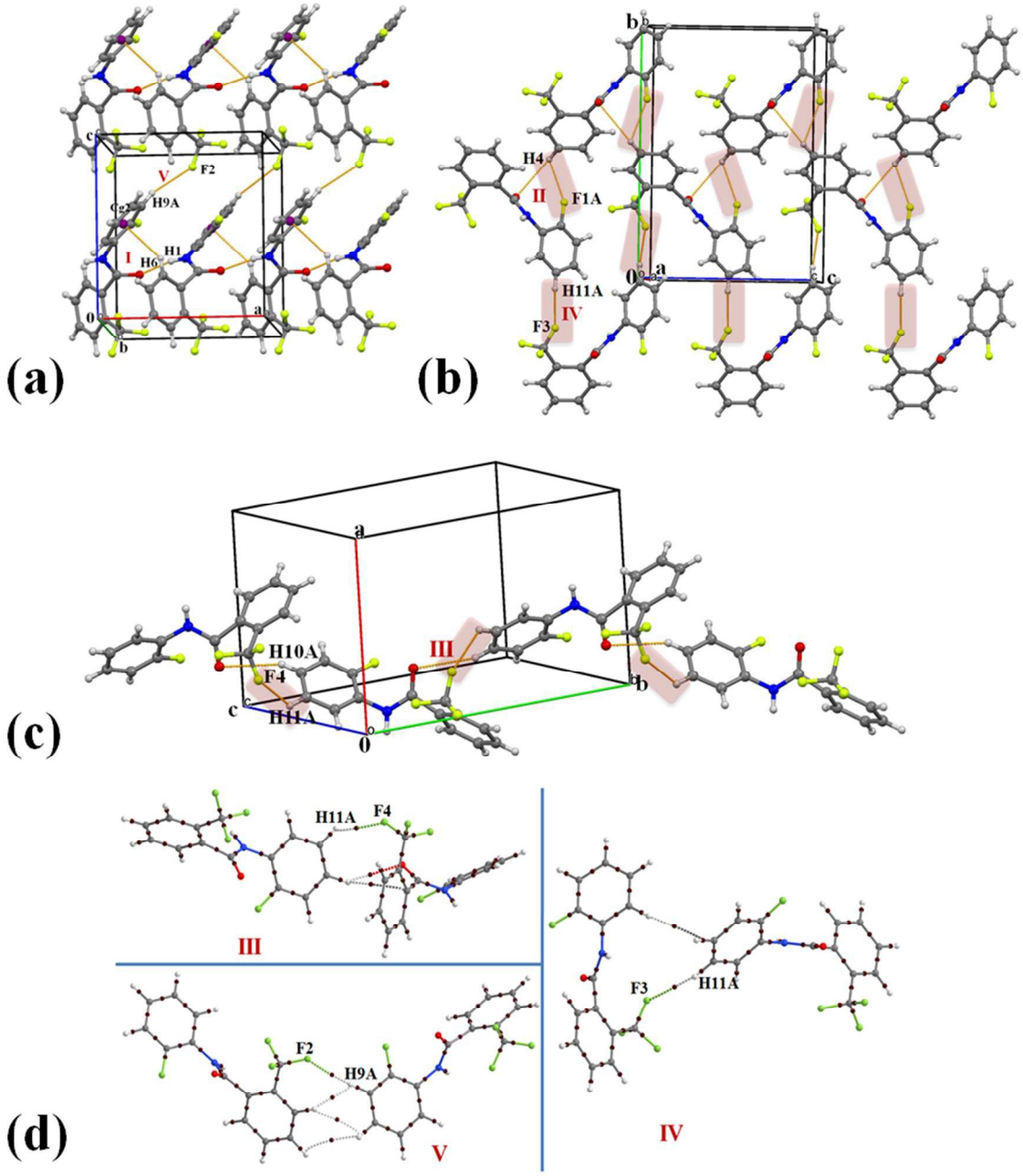

Figure 1(a): Packing of molecules in **1F1T** *via* the network of strong N-H···O=C, weak C-H···π and C-H···F-C_{sp3} hydrogen bonds. The Roman numbers in red (in this and also subsequent diagrams) indicate the molecular motifs presented in the **Table S3**. **(b)** Formation of the herringbone layer of molecules down the *bc* plane with the utilization of weak C-H···O, C-H···F-C_{sp2} and C-H···F-C_{sp3} hydrogen bonds in **1F1T**. **(c)** Formation of the molecular chain in **1F1T** *via* weak C-H···O and C-H···F-C_{sp3} hydrogen bonds. **(d)** Selected molecular motifs (denoted with Roman number from **Table S4**) in **1F1T**, showing different intermolecular interactions. The brown small spheres represent bond critical points (BCPs) on the bond path.

2) *N*-(3-fluorophenyl)-2-(trifluoromethyl)benzamide (2F1T):

The compound **2F1T** crystallizes in the monoclinic centrosymmetric space group $P2_1/c$ with three molecules in the asymmetric unit (Z' = 3) (**Fig 2**). Two (molecule **2** and **3**) out of three molecules in the asymmetric unit observed in the formation of the most stabilized molecular motif **I** (-13.3 kcal/mol) involving strong N-H···O=C, weak C-H···π and C-H···F-C_{sp3} hydrogen bonds along with π···π interactions. Selected molecular pairs, which contribute towards the stabilization of the crystal packing in **2F1T**, are presented in **Figure 2(c)** along with their interaction energies (I.E). The three most stabilized molecule motifs **I**, **II** (-13.1 kcal/mol) and **III** (-12.2 kcal/mol), consisting of strong N-H···O=C hydrogen bond along with other weak interactions (**Table S3a**) were observed to be involved in the formation of a molecular chain along the crystallographic *a*-axis in the crystal packing [**Fig. 2(a)** and **(b)**]. Such chains were observed to be connected with the utilization of the motif **IV**, **V** and **VII** in the crystal packing [**Fig. 2(a)**]. The motif **IV** (I.E = -5.3 kcal/mol) consists of short C-H···O=C (2.39Å/ 149°) and C-H···π (2.68Å/ 141°) hydrogen bond while the motif **V** (-4.7 kcal/mol) involves the presence of weak C-H···F-C_{sp3} hydrogen bond [**Fig. 2(a)**] along with π···π interactions. A short C-H···F-C_{sp3} (2.39Å/ 127°) and a weak C-H···π (2.86Å/ 155°) hydrogen bond were recognized to connect the molecules in motif **VII**. Moreover, the packing of molecules in **2F1T** are also stabilized by the presence of weak C-H···F-C_{sp2} hydrogen bond in the motifs **VIII**, **IX** and **XI** with the stabilization energy ranging from -1.3 to -2.6 kcal/mol [**Table S3, Fig. 2(c)**]. It is to be noted that the motif **X**, involves the presence of bifurcated C_{sp2}-F···F-C_{sp3} interactions [*Type I* (2.883Å, 110°, 94°) and other a "*near*" *Type II* (3.133Å, 152°, 83°) contact], provides stabilization towards the crystal packing with interaction energy of 1.7 kcal/mol, the nature being primarily of dispersive origin. A very recent charge density analysis has revealed the polarization of the electron density on the fluorine atoms on the trifluoromethyl group which facilitate the formation of type II C-F···F-C contacts in the crystal **[67]**. Furthermore, a very short *type I* C_{sp2}-F···F-C_{sp3} interaction [2.736Å, 146°, 149°, motif **XII**] were observed in the crystal packing, providing almost negligible stabilization [0.1 kcal/mol] [**Fig. 2(c)**]. This stabilization energy is similar with the value reported in a recent analysis by *ab initio* calculations on all the unique dimers, extracted from the crystal structure of CF_4, C_2F_4 and C_6F_6 by Osuna *et al.* **[68]**.

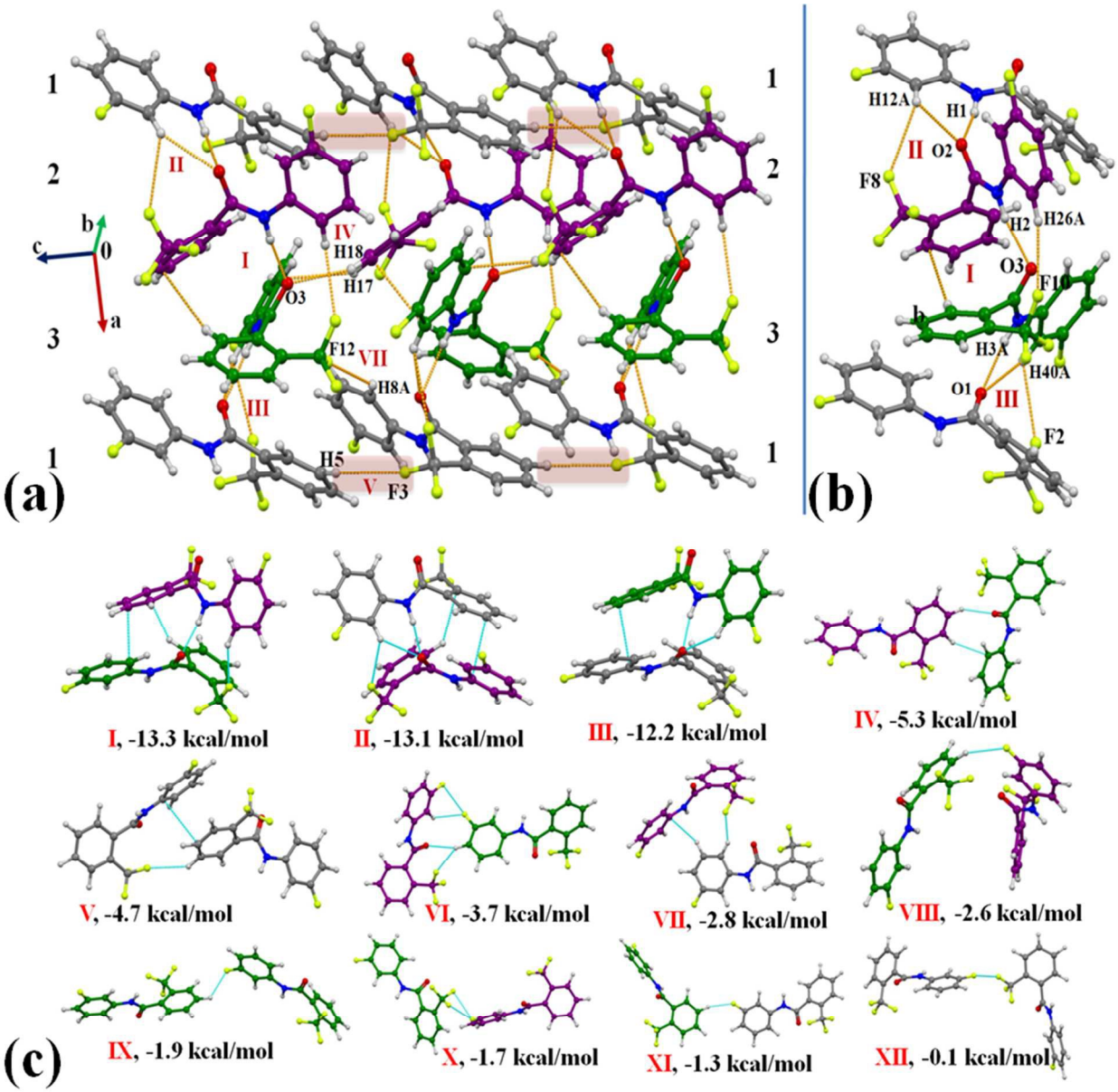

Figure 2(a): Packing of molecules in **2F1T** *via* the network of strong N-H···O=C, weak C-H···π and C-H···F-C_{sp3} hydrogen bonds. **(b)** Clear depiction of the …123… molecular chain along the crystallographic *a*-axis. Different color codes of carbon atoms indicate the presence of three molecules in the asymmetric unit. Grey: Molecule 1, Purple: Molecule 2 and Green: Molecule 3. **(c)** Selected molecular pairs extracted from the crystal packing of **2F1T** along with their interaction energies (**Table S3**).

3) *N*-(2-fluorophenyl)-3-(trifluoromethyl)benzamide (1F2T):

The compound **1F2T** crystallizes in the monoclinic centrosymmetric space group with $Z = 4$. **Figure 3(a)** depicts the packing of molecules in **1F2T** in all the three directions with the utilization of different molecular motifs **I** to **VIII** (**Table 2**). The highest stabilized molecular motif **I** (I.E = -11.8 kcal/mol) consists of strong N-H···O=C, a short and directional C-H···F-C_{sp2} (2.47Å, 168°) and a short C-H···π (2.66Å, 158°) hydrogen bond along with a C-F···π interactions. The motif **I** along with motif **III** [I.E = -4.8 kcal/mol; consists of a short C-H···π (2.61Å, 159°) and C-H···O=C hydrogen bond] and motif **V** (I.E = -1.9 kcal/mol; involves a bifurcated C-H···F-C_{sp3} along with the presence of C-F···π interactions) were observed to pack the molecules along the *c*-axis with the utilization of *c*-glide perpendicular to *b*-axis. A short and directional C-H···F-C_{sp2} (2.45Å, 168°) hydrogen bond along with the two π···π interactions in the motif **II** (-6.4 kcal/mol) were observed to connect the molecules along the crystallographic *a*-axis. The molecular chains, formed along the *a*-axis, with the utilization of motif II [**Fig. 3(b)**], were observed to be connected *via* motifs **IV**, **VI** to **VIII** in the generation of a molecular layer down the *ab* plane. Amongst these, motif **VI** (-1.5 kcal/mol) and **VII** (-1.1 kcal/mol) were found to consist of a short C-H···F-C_{sp3} (2.47Å, 161°; 2.57Å, 139°) hydrogen bond while the motif **IV** (I.E = -2.0kcal/mol), involves dimeric C_{sp3}-F···F-C_{sp3} interaction and a weakly stabilized (-0.2 kcal/mol) motif **VIII** consists of *type I* C_{sp3}-F···F-C_{sp3} (2.942Å, 158°, 158°) interactions. Further, QTAIM calculations, reveal the presence of a (3, -1) BCP for all C-H···F and C-F···F-C interactions [**Fig. 3(c)**].

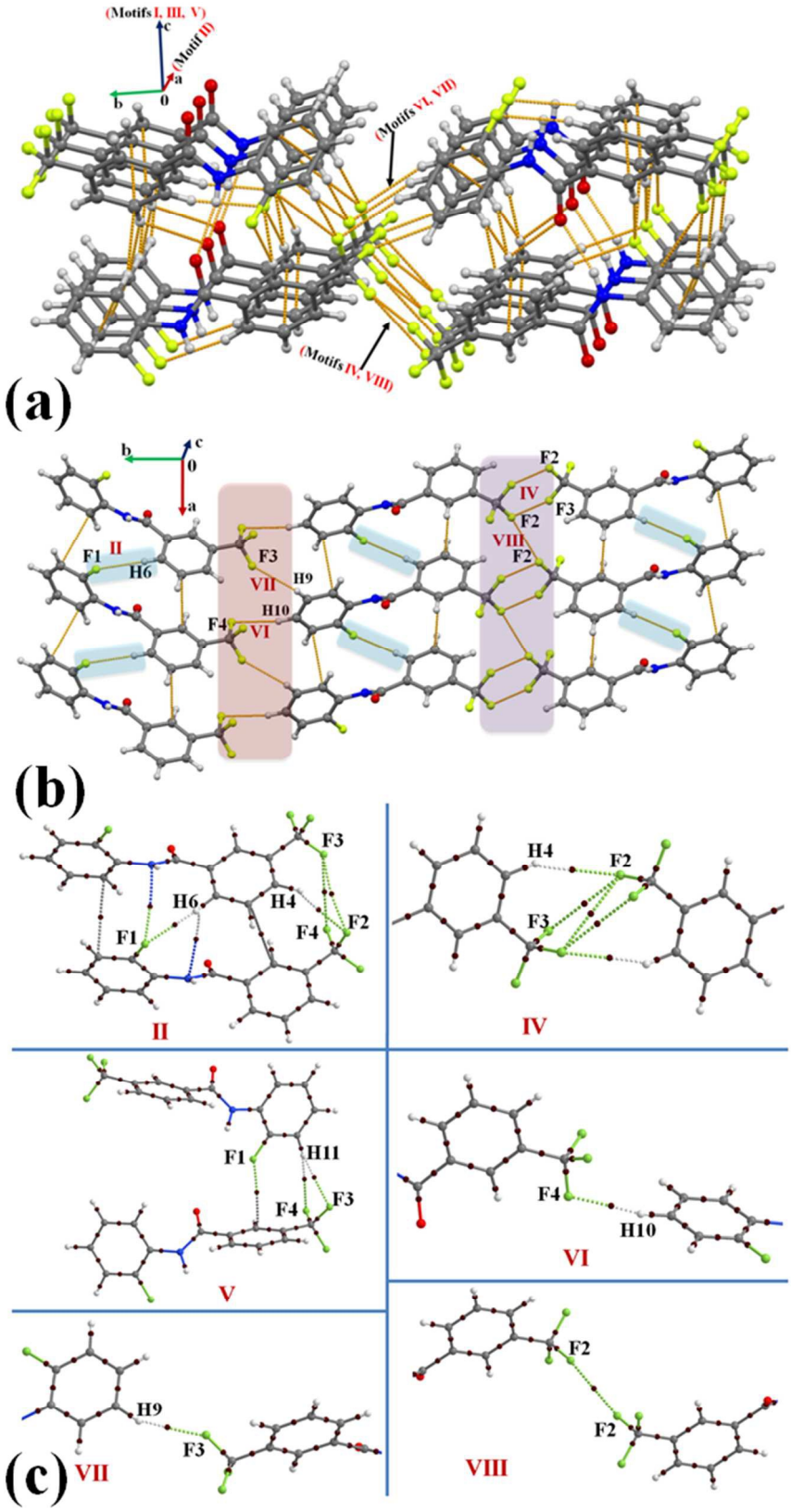

Figure 3(a): Packing of the molecules down the *bc* crystallographic plane in **1F2T** *via* the network of strong N-H···O=C, weak C-H···π, C-H···F-C_{sp2} and C-H···F-C_{sp3} hydrogen bonds along with π···π, C_{sp3} -F···π and C_{sp3} -F···F- C_{sp3} interactions. **(b**) Part of the crystal packing in **1F2T** down the *ab* plane, displaying the presence of weak C-H···F-C_{sp2} and C-H···F-C_{sp3} hydrogen bonds along with π···π (off set) and C_{sp3} -F···F-C_{sp3} interactions. **(c)** Selected molecular motifs (denoted with Roman number from **Table S4**) in **1F2T**, showing different intermolecular interactions. The small brown spheres represent bond critical points (BCPs) on the bond path. Only the interacting part of the motifs was shown in case of **IV**, **VI – VIII.**

4) *N*-(3-fluorophenyl)-3-(trifluoromethyl)benzamide (2F2T):

The compound **2F2T** crystallizes in the orthorhombic centrosymmetric space group *Pbcn* with Z = 8. The most stabilized molecular motif **I** (I.E = -12.1 kcal/mol) consists of strong N-H···O=C hydrogen bond supported by weak C-H···O, and C-H···π hydrogen bonds. A molecular chain, formed *via* motif **I** utilizing *c*-glide, were observed to connect *via* the weak C-H···π hydrogen bonds recognized in the motif **II** (-4.2 kcal/mol), **VI** (-2.1 kcal/mol), **VIII** (-1.6 kcal/mol) [**Fig 4(a)**]. Furthermore, packing of molecules in **2F2T** were stabilized by the formation of motifs **III** (-3.0 kcal/mol) and **IV** (-2.4 kcal/mol)**,** comprising of dimeric weak C-H···F-C_{sp3} hydrogen bonds. It is of interest to note that a short and directional C_{sp3} -F···π [3.134Å, 150°, **Table S3**] interaction, utilizing 2 fold rotation parallel to *b*-axis, provided (motif **V**) stabilization to the crystal packing [2.3 kcal/mol] with dispersion being a major contributor. Moreover, a bifurcated weak C-H···F-C_{sp2} hydrogen bonds (motif **VII**, -1.7 kcal/mol) were realized in the formation of a molecular chain, utilizing a *c*-glide plane perpendicular to the *b*-axis. Such chains were connected with the presence of motif **IX** (-0.2 kcal/mol), possessing a pair of weak *type I* C_{sp3} -F···F-C_{sp3} interactions including the one at short distance (2.873Å, 122°, 122°) [**Fig. 4(b)**]. It was also noticed that the two sides of the phenyl ring, substituted with the fluorine and $–CF_3$ group, were observed in the formation of different supramolecular motifs in the crystal packing [**Fig. 4(c)**].

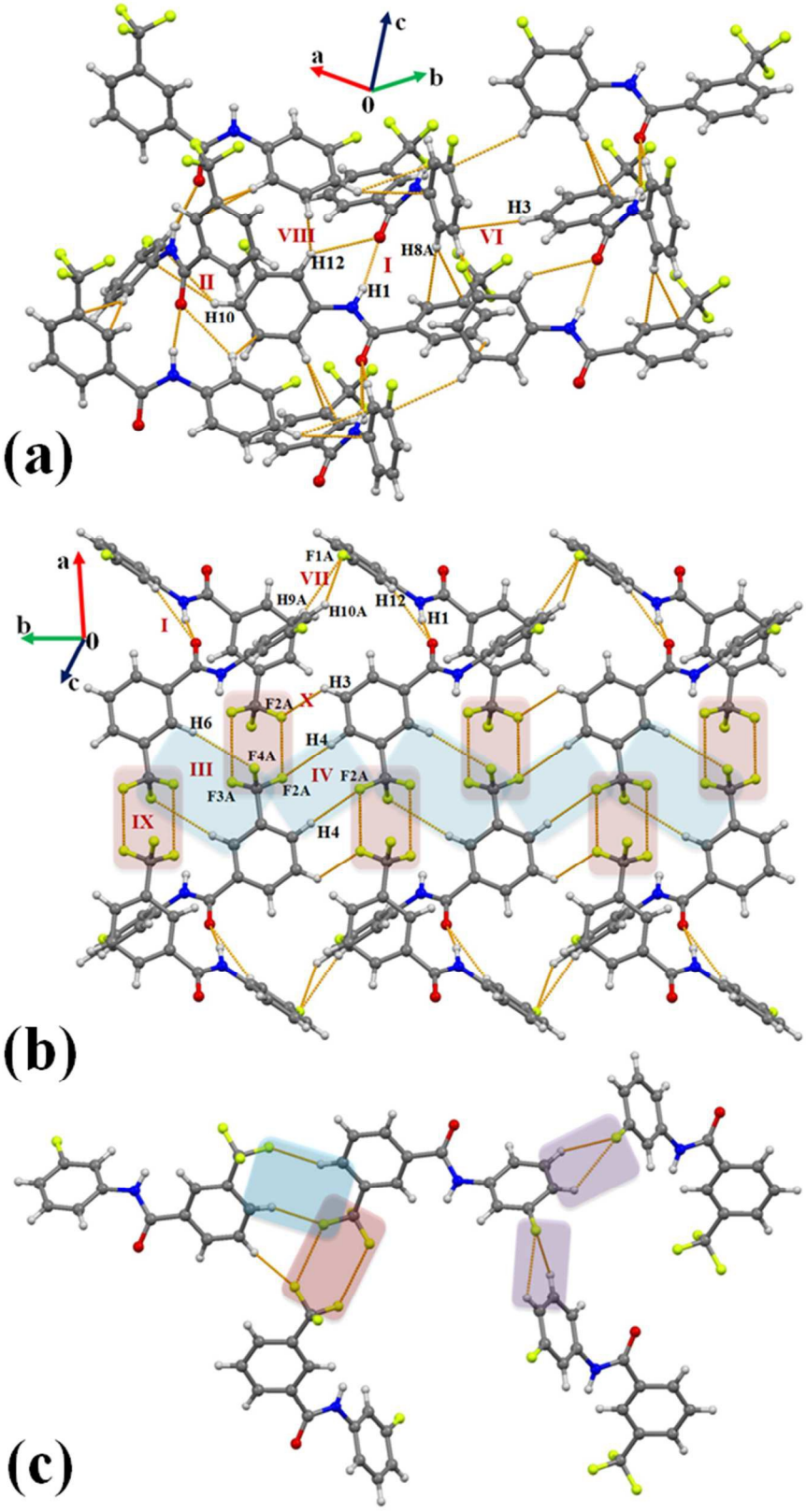

Figure 4(a): Packing of molecules in **2F2T** *via* the network of strong N-H···O=C, weak C-H···O, C-H···π hydrogen bonds. **(b)** Packing of molecules in **2F2T**, displaying the network of strong N-H···O=C, weak C-H···O, C-H···F-C_{sp2} and C-H···F-C_{sp3} hydrogen bonds along with C_{sp3}-F···F-C_{sp3} interactions. **(c)** Part of crystal packing in **2F2T**, depicting the presence of different motifs involving fluorine interactions.

5) *N*-(3-fluorophenyl)-4-(trifluoromethyl)benzamide (2F3T):

The compound **2F3T** was found to crystallize in the monoclinic centrosymmetric space group *C*2/*c* with Z = 8. The strong N- H···O=C hydrogen bond along with the weak C-H···O=C hydrogen bond and π···π interactions (Motif **I**, -12.3 kcal/mol) was observed to engage in the formation of molecular chains along the crystallographic *b*-axis. Such chain is connected by the utilization of weak C-H···π hydrogen bonds and π···π interactions in the formation of a molecular layer down the *bc* plane [**Fig. 5(a)**], involved in the next three stabilized motifs **II** (-7.6 kcal/mol), **III** (-7.4 kcal/mol) and **IV** (-6.1 kcal/mol). Packing of molecules down the *bc* plane [**Fig. 5(b)**] was detected as the formation of a molecular sheet with utilization of bifurcated weak and short C-H···F-C_{sp3} hydrogen bonds [2.55Å, 145° (motif **VIII**, -1.3 kcal/mol); 2.55Å, 125° (motif **IX**, -1.1 kcal/mol)], along the *b*-axis. Furthermore, the crystal packing of **2F3T** was also observed to be stabilized by the formation of similarly stabilized molecular motifs **V** (-2.2 kcal/mol) and **VI** (-2.1 kcal/mol) [**Fig. 5(c)**]. The motif **V** consists of bifurcated weak C-H···F-C_{sp2} hydrogen bonds while the motif **VI** involves in the formation of dimeric C_{sp3}-F···F-C_{sp3} interactions. In addition, a *type II* C_{sp3}-F···F-C_{sp3} interaction (motif **VII**, -1.9 kcal/mol) were also observed to form a chain, utilizing 2_1 screw axis along the crystallographic *b*-axis in the crystal packing [**Fig. 5(d)**]. The selected motifs, containing weak C-H···F and C_{sp3}-F···F-C_{sp3} interactions, were characterized by the QTAIM theory and the presence of (3, -1) BCPs were observed on the bond path of these interactions [**Fig. 5(e)**, **Table S5**].

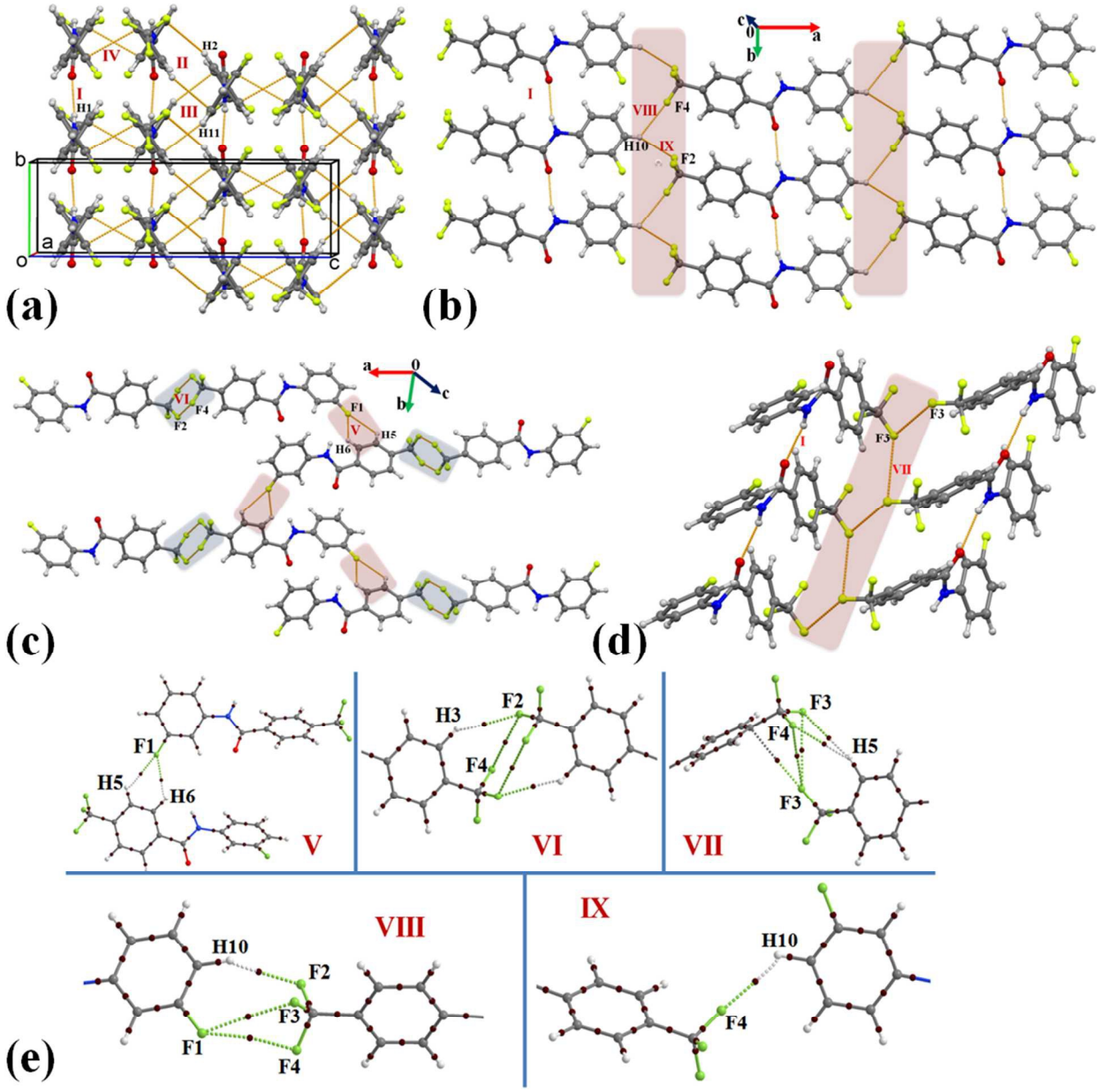

Figure 5(a): Formation of a molecular layer down the *bc* crystallographic plane with the utilization of strong N-H···O=C, weak C-H···π hydrogen bonds and π···π interactions in **2F3T**. **(b)** Packing of molecules down the *ab* plane *via* the networks of strong N-H···O=C and weak C-H···F-C_{sp3} hydrogen bonds in **2F3T**. **(c)** Part of the crystal packing in **2F3T**, displaying the formation of bifurcated weak C-H···F-C_{sp2} hydrogen bonds and dimeric C_{sp3}-F···F-C_{sp3} interactions. **(d)** Part of the crystal packing **2F3T** showing the presence of C_{sp3}-F···F-C_{sp3} interactions forming a chain motif along with a strong N-H···O=C hydrogen bond. **(e)** Selected molecular motifs (**Table S4**) in **2F3T**, showing different intermolecular interactions. The small brown spheres represent bond critical points (BCPs) on bond path. Only interacting part of the motif was shown in case of **VI - IX**.

6) *N*-(4-fluorophenyl)-4-(trifluoromethyl)benzamide (3F3T):

The compound **3F3T** crystallizes in the triclinic centrosymmetric space group *P*-1 with *Z* = 2. As expected, the most stabilized molecular motif **I** (-11.7 kcal/mol) was noticed to involve strong N-H···O=C hydrogen bond along with weak C-H···O=C hydrogen bond and π···π interactions. The motif **I** was found to involve in the formation of molecular chain along the crystallographic *a*-axis. Such chains were interlinked *via* dimeric weak C-H···F-C_{sp2} hydrogen bonds [motif **VII** (-1.4 kcal/mol) and **VIII** (-1.1 kcal/mol)] and dimeric weak C_{sp3}-F···F-C_{sp3} interactions [motif **IX** (-0.7 kcal/mol)] in the formation of a molecular layer down the *ab* plane. Further, in the molecular packing of **3F3T**, the molecular chains formed with the utilization of motif **VIII** and **IX**, were observed to be connected by the molecular motifs **II** to **VI** which consist of other weak interactions in the crystal packing [**Fig. 6(b)**]. The motif **II** involves the presence of a weak C-H···π hydrogen bond and a short C_{sp3}-F···O=C (3.118Å, 120°) interaction, the interaction energy being -6.1 kcal/mol. The motif **III** and **IV** were noticed to provide similar stabilization towards the crystal packing (-4.7 kcal/mol and -4.0 kcal/mol respectively) but observed to involve different interactions. The motif **III** consist of weak C-H···F-C_{sp3} and C-H···π hydrogen bonds while the weak π···π interaction was observed in motif **IV**. Moreover, a dimeric short C-H···F-C_{sp3} (2.45Å, 157°) contact were observed to stabilize (motif **V**, -2.8 kcal/mol) the crystal packing in **3F3T**. In addition, a dimeric weak C_{sp3}-F···π interactions (motif VI, -2.2 kcal/mol) were also observed to provide stabilization to the crystal packing in **3F3T**. The weak interactions involving fluorine in **3F3T** were studied with QTAIM theory and the presence of (3, -1) BCP were observed for these interactions in their corresponding molecular motifs [**Fig. 6(c)**].

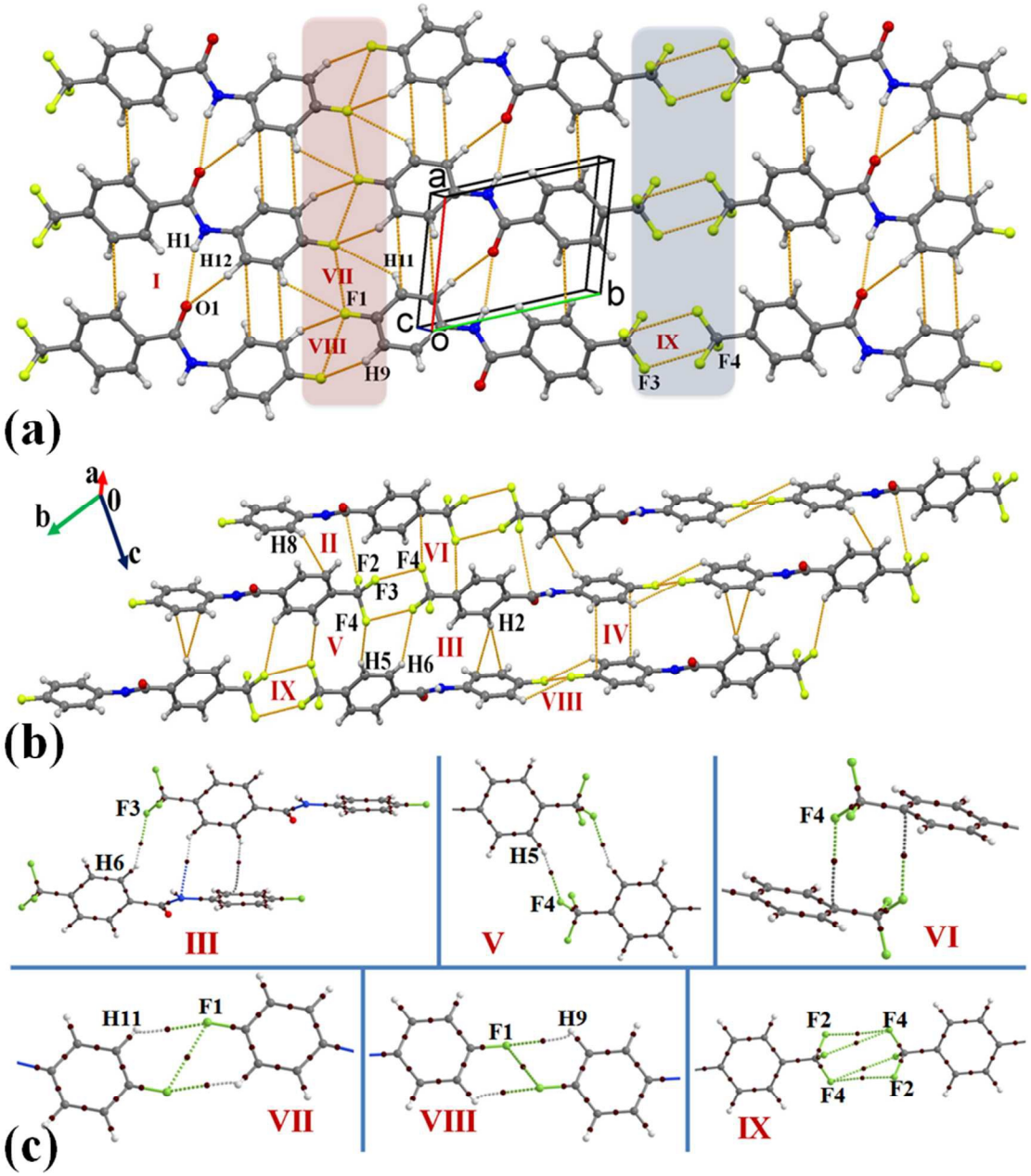

Figure 6(a): Packing of molecules in **3F3T** down the *ab* crystallographic plane with the utilization of strong N-H···O=C, weak C-H···O=C, C-H···F-C_{sp2} hydrogen bonds along with C_{sp2}-F···F-C_{sp2}, C_{sp3}-F···F-C_{sp3} and π···π interactions. **(b)** Packing of molecules in **3F3T** down the *bc* crystallographic plane *via* weak C-H···F-C_{sp2}, C-H···F-C_{sp3} and C-H···π hydrogen bonds along with C_{sp2}-F···F-C_{sp2}, C_{sp3}-F···F-C_{sp3}, C_{sp3}-F···O=C, C_{sp3}-F···π and π···π interactions. **(c)** Selected molecular motifs (**Table S4**) in **3F3T**, showing different intermolecular interactions. The small brown spheres represent bond critical points (BCPs) on bond path. Only interacting part of the motif was shown in case of **III, V – VII, IX** and **X**.

7) 2-fluoro-*N*-(3-(trifluoromethyl)phenyl)benzamide (2T1F):

The compound **2T1F** crystallizes in the centrosymmetric orthorhombic space group *Pbca* with *Z* = 8. A strong N-H···O=C hydrogen bond along with π···π interactions (motif **I**, **-11.6** kcal/mol check this value) was observed in the generation of a *zig-zag* chain with the utilization of *b*- glide perpendicular to the *a*-axis. The chains are interconnected utilizing motif **VII** which consist of the weak near *type II* C_{sp3}-F···F-C_{sp3} (2.990Å, 108°, 154°) interactions (I.E. being -1.0 kcal/mol). The next most stabilized motif **II** (-4.5 kcal/mol), consisting of weak π···π interaction, was found to connect the molecular chain [**Fig. 7(b)**] generated *via* 2_1-screw along *b*-axis utilizing weak C-H···π hydrogen bond (Motif **V**, -2.8 kcal/mol). Furthermore, there was formation of a herringbone pattern down the *ac* plane [**Fig. 7(c)**] observed in the crystal packing of **2T1F**, exploiting motif **III**, **IV** and **VI**. The motif **III** (-3.0 kcal/mol) was noticed to involve weak C-H···O and C-H···F-C_{sp3} hydrogen bond while it was short bifurcated C-H···F-C_{sp2} hydrogen bonds which were observed in the motif **IV**, the stabilization energy being 2.8 kcal/mol. Moreover, a weak C-H···F-C_{sp3} hydrogen bond was recognized in the motif **VI** (-1.4 kcal/mol).

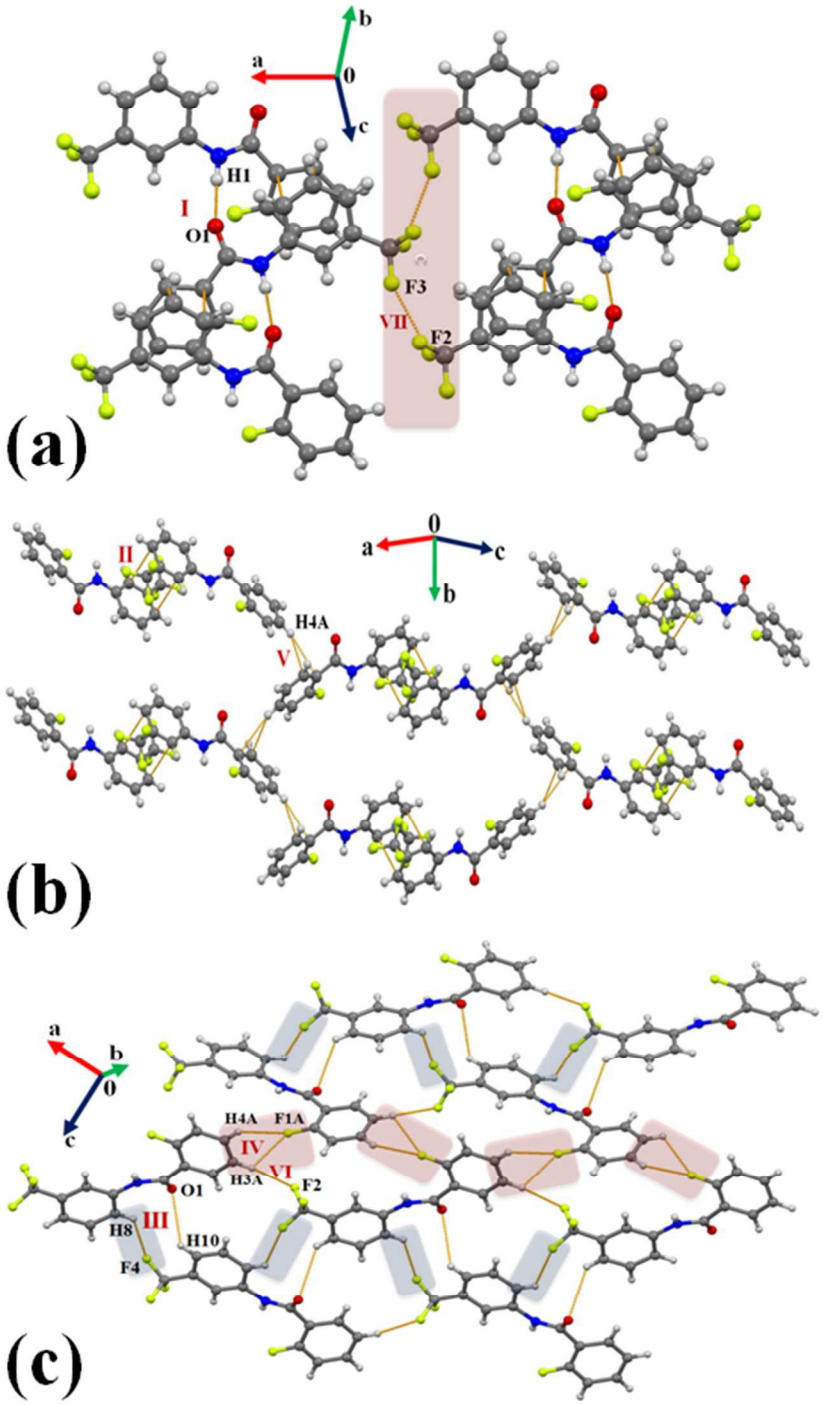

Figure 7(a): Packing of molecules in **2T1F** *via* strong N-H···O=C hydrogen bonds along with C_{sp3}-F···F-C_{sp3} and π···π interactions. **(b)** Packing of molecules in **2T1F** *via* the network of weak C-H···π hydrogen bonds and π···π interactions. **(c)** Formation of a molecular layer in **2T1F** down the *ac* crystallographic plane with the utilization of *via* weak C-H···O, C-H···F-C_{sp2} and C-H···F-C_{sp3} hydrogen bonds.

8) 2-fluoro-*N*-(3-(trifluoromethyl)phenyl)benzamide hydrate (2T1F_w):

Hydrate of the compound 2-fluoro-*N*-(3-(trifluoromethyl)phenyl)benzamide hydrate (**2T1F_w**) crystallizes in the orthorhombic centrosymmetric space group *Pbcn* with half molecule of water in the asymmetric unit (**Table S2**). It has been characterized using differential scanning calorimetry (DSC), thermal gravimetry analysis (TGA) and hot stage microscopy (HSM) (**Section S3** in ESI). Packing of the molecules in **2T1F_w** were observed to be stabilized by the solvent molecule with the formation of strong hydrogen bonds like N-H···O_{water} and O_{water}-H···O=C, noticed in motif **I** and **II** with I.E. being -5.04 kcal/mol and -5.63 kcal/mol respectively [**Table S3c, Fig. 8(a)**]. A stacked motif **III** along *a*- axis (utilizing 2_1-screw), consisting of two weak C-H···F-C_{sp3} hydrogen bonds along with π···π interactions, is a highly stabilized (-14.2 kcal/mol) molecular pair in the crystal packing [**Fig 8(a)**, **Table S3c**]. The packing of the molecules down the *bc* plane shows the formation of a molecular layer utilizing the motif **I**, **II**, **IV** and **V** [**Fig 8(b)**]. The molecular chain with alternate interactions of the compound and solvent was observed to be connected with weak C-H···F-C_{sp3} hydrogen bond (motif **V**, -1.64 kcal/mol) utilizing *c*-glide perpendicular to *b*-axis [**Fig. 8(b)**]. Moreover, the presence of highly short *type I* C_{sp3}-F···F-C_{sp3} interactions were recognized in the weakly stabilized molecular motif **VI** (-0.42 kcal/mol) and relatively destabilized motif **VII** (+1.29 kcal/mol) (**Table S3c**). It is to be noted here that the molecules in the destabilized motif **VII**, consisting of highly short *type I* C_{sp3}-F···F-C_{sp3} interactions (2.663Å, 132°, 132°), was observed to be stabilized by the presence of water molecule *via* the formation of two strong O_{water}-H···O=C hydrogen bonds (motif **II**) in the crystal packing [**Fig. 8(a)**].

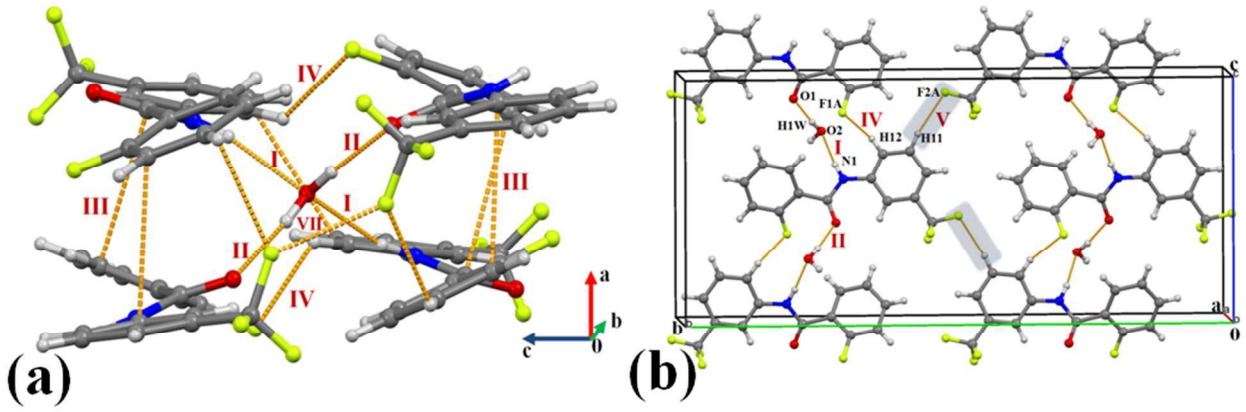

Figure 8(a): Part of the crystal packing in **2T1F_w**, displaying formation of strong N-H···O_{water} and O_{water}-H···O=C, weak C-H···F-C_{sp3} hydrogen bond along with C_{sp3}-F···F-C_{sp3} and π···π interactions. **(b)** Packing view down the *bc* plane in **2T1F_w**, displaying formation of molecular layer utilizing interactions involving the solvent along with C-H···F-C_{sp3} hydrogen bonds.

9) 2-fluoro-*N*-(4-(trifluoromethyl)phenyl)benzamide (3T1F):

The compound **3T1F** crystallizes in the non-centrosymmetric orthorhombic space group $P2_1cn$ with Z = 4. Packing of molecules in **3T1F** involve the formation of a molecular chain along the *b*- axis with the utilization of strong N-H···O=C along with weak C-H···O=C hydrogen bond and π···π interactions (motif **I**, -9.7 kcal/mol, **Table S3**). Such chains are interconnected by the utilization of next two similarly stabilized motifs **II** (-6.5 kcal/mol) and **III** (-6.3 kcal/mol) in the formation of a molecular layer down the (101) plane [**Fig. 9(a)**]. The motif **II** involved a pair of weak C-H···π hydrogen bonds along with a short C_{sp3}-F···F-C_{sp3} (2.840Å, 127°, 171°) and a short C_{sp2}-F···C=O (3.134Å, 146°) interactions (**Table S3**) whereas a short and directional C-H···π (2.65Å, 156°) and C-H···F-C_{sp3} (2.56Å, 160°) hydrogen bonds were present in motif **III**. Furthermore, a molecular chain formed by the utilization of bifurcated C-H···F-C_{sp3} hydrogen bonds (motif **IV**, -1.9 kcal/mol, 2_1 screw parallel to *a*-axis) were observed to be interconnected *via* the motif **II**, **III** and **V** in the packing of molecules down the *ac* plane in **3T1F**. The motif **V** (-1.6 kcal/mol) was found to consist of weak C-H···F-C_{sp3} hydrogen bonds. These were presence of (3, -1) BCPs identified in case of weak C-H···F and C-F···F-C interactions [**Fig. 9(c)**, **Table S4**].

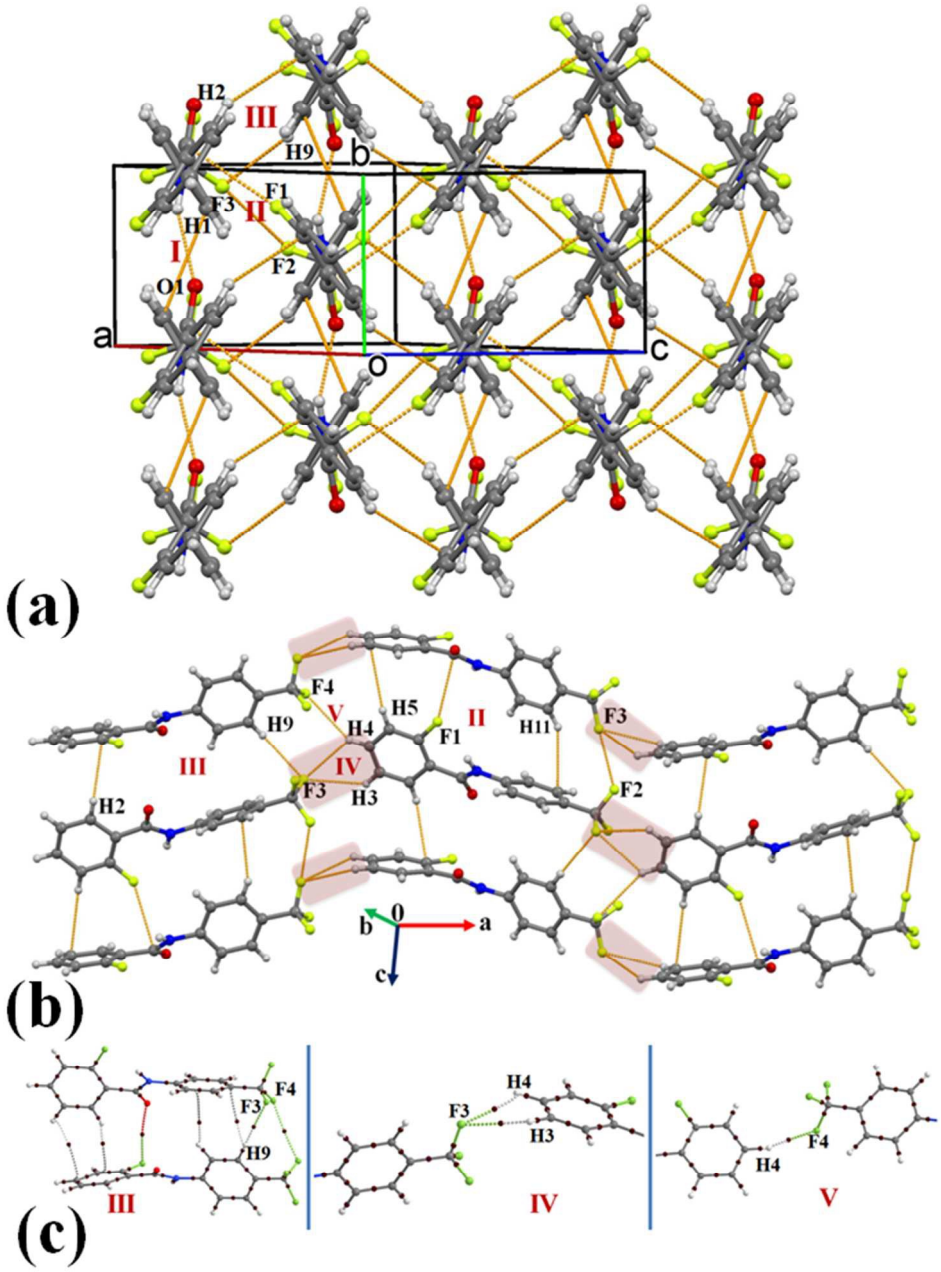

Figure 9(a): Packing of molecules in **3T1F** *via* the network of strong N-H···O=C, weak C-H···π, and C-H···F-C_{sp3} hydrogen bonds along with C_{sp3}-F···F-C_{sp3}, C_{sp2}-F···C=O and π···π interactions. **(b)** Packing view down the *ac* plane in **3T1F** *via* the network of weak C-H···π and C-H···F-C_{sp3} hydrogen bonds along with C_{sp3}-F···F-C_{sp3}, C_{sp2}-F···C=O interactions. **(c)** Selected molecular motifs (**Table S4**) in **3T1F**, showing different intermolecular interactions. Only interacting part of the motif was shown in case of **IV – V**.

10) 3-fluoro-*N*-(2-(trifluoromethyl)phenyl)benzamide (1T2F):

The compound **1T2F** crystallizes in the centrosymmetric monoclinic space group $P2_1/c$ with two molecules in the asymmetric unit (Z = 8). The two most and similarly stabilized molecular motifs **I** (-12.9 kcal/mol) and **II** (-12.4 kcal/mol) were observed to consist of strong N-H···O=C hydrogen bond along with short C_{sp3}-F···C=O (3.090Å, 141°; 3.011Å, 141° respectively, **Table S3**) and π···π interactions. These motifs were appeared to be involved in the formation of …*1212*… type molecular chain along the crystallographic *a*-axis. Such chains are recognized to interlink with the exploitation of next four stabilized molecular motifs **III**, **IV**, **V** and **VI**. In the similarly stabilized motifs **III** (-4.6 kcal/mol) and **IV** (-4.4 kcal/mol), there were short and directional C-H···O=C (2.33Å, 149°; 2.23Å, 168°) hydrogen bonds recognized with contribution from electrostatic (Coulombic + Polarization) was significant (46% and 54% respectively). Further, the motif **V** (involving a bifurcated weak C-H···F-C_{sp3} and C-H···π hydrogen bonds) and **VI** (involving a bifurcated weak C-H···F-C_{sp3} hydrogen bond) were observed to provide similar stabilization (-3.5 and -3.2 kcal/mol respectively) to the crystal packing. Moreover, inter molecular interactions involving organic fluorine of type C-H···F, C-F···F-C were noticed to stabilize the crystal packing in **1T2F** and participate in the generation of different supramolecular motifs **VII** to **XII** (**Table S3**) in the crystal packing [**Fig. 10(b)** & **10(c)**]. The motif **VII (**-2.8 kcal/mol**)** was observed to be composed of a dimeric weak C-H···F-C_{sp3} hydrogen bonds along with dimeric C_{sp3}-F···F-C_{sp3} interactions while a dimeric weak C-H···F-C_{sp2} hydrogen bond, interacting side wise, was recognized in the equally stabilized motif **VIII**. Further, a bifurcated weak C-H···F-C_{sp3} hydrogen bond was observed in motif **IX (**-1.8 kcal/mol**)** whereas in the similarly stabilized motif **X** (-1.7 kcal/mol), a short C-H···F-C_{sp2} hydrogen bond (2.48Å, 137°) was recognized. In the last two weakly stabilized motifs **XI** (-1.1 kcal/mol) and **XII** (-0.6 kcal/mol), a weak C-H···F-C_{sp2} hydrogen bond and weak type I C_{sp3}-F···F-C_{sp2} interactions were observed respectively. All the molecular pairs consisting of weak C-H···F and C-F···F-C interactions were analyzed by the theory of QTAIM and the topological parameters were obtained (**Table S4**). There was presence of (3, -1) BCPs noticed for these interactions along with other related contacts in the respective motifs [**Fig. 10(d)**].

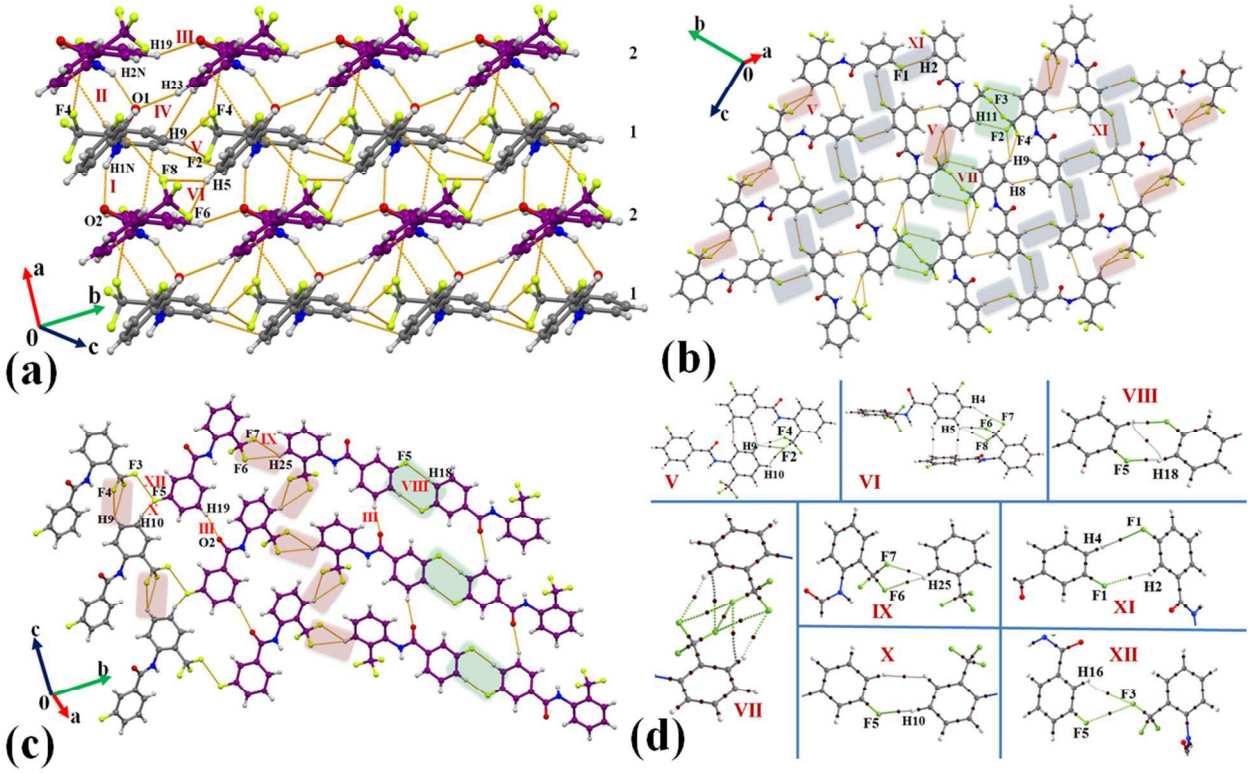

Figure 10(a): Formation of *…1212…* type molecular layer in **1T2F** *via* strong N-H···O=C, weak C-H···O, C-H···π, and C-H···F-C_{sp3} hydrogen bonds along with C_{sp3}-F···C=O and π···π interactions. C-atoms in purple are shown for the second molecule in the asymmetric unit. **(b)** Packing view down the *bc* plane, displaying network of weak C-H···π, C-H···F-C_{sp2}, C-H···F-C_{sp3} hydrogen bonds along with C_{sp3}-F···F-C_{sp3} interactions in **1T2F**. **(c)** Packing of molecules in **1T2F** via network of weak C-H···O, C-H···F-C_{sp2}, C-H···F-C_{sp3} hydrogen bonds along with C_{sp3}-F···F-C_{sp3} interactions. C-atoms in purple are shown for the second molecule in the asymmetric unit. **(d)** Selected molecular motifs (**Table S4**) in **1T2F**, showing different intermolecular interactions. Only interacting part of the motif was shown in case of **VII – XII**.

11) 3-fluoro-*N*-(3-(trifluoromethyl)phenyl)benzamide (2T2F):

The compound **2T2F** crystallizes in the non-centrosymmetric monoclinic space group *Cc* with four molecules in the unit cell. A strong N-H···O=C hydrogen bond along with π···π interactions (motif **I**, -11.3 kcal/mol) steer the molecules along [110] in the formation of a molecular chain. Such chains are interlinked with the involvement of next two stabilized motifs **II** (-5.5 kcal/mol) and **III** (-4.8 kcal/mol) in the crystal packing. The motif **II** was recognized to involve weak π···π interactions with substantial contribution from dispersion energy towards the total stabilization whereas a weak C-H···O=C along with two short C-H··· F-C_{sp2}/C_{sp3} (2.45Å, 133°; 2.53Å, 136°

respectively) hydrogen bonds were observed in motif **III**. Further the molecular ladder formed *via* the motif **III** was observed to be connected by the utilization of motifs **IV**, **V** and **VI** in the crystal packing [**Fig. 11(b)** & **11(c)**]. The motif **IV** (-2.2 kcal/mol) consists of bifurcated weak C-H··· F-C_{sp3} hydrogen bonds while a short C-H···F-C_{sp3} (2.50Å, 146°) hydrogen bond was observed in motif **V** (-1.5 kcal/mol). Moreover, a weak *type I* C_{sp3}-F···F-C_{sp3} interaction (motif **VI**, -1.2 kcal/mol) was also recognized to stabilize the packing the molecules in **2T2F** (**Table S3**). The presence of (3, -1) BCPs were observed for the weak C-H···F and C-F···F-C interactions in the respective motifs [**Fig. 11(d)**].

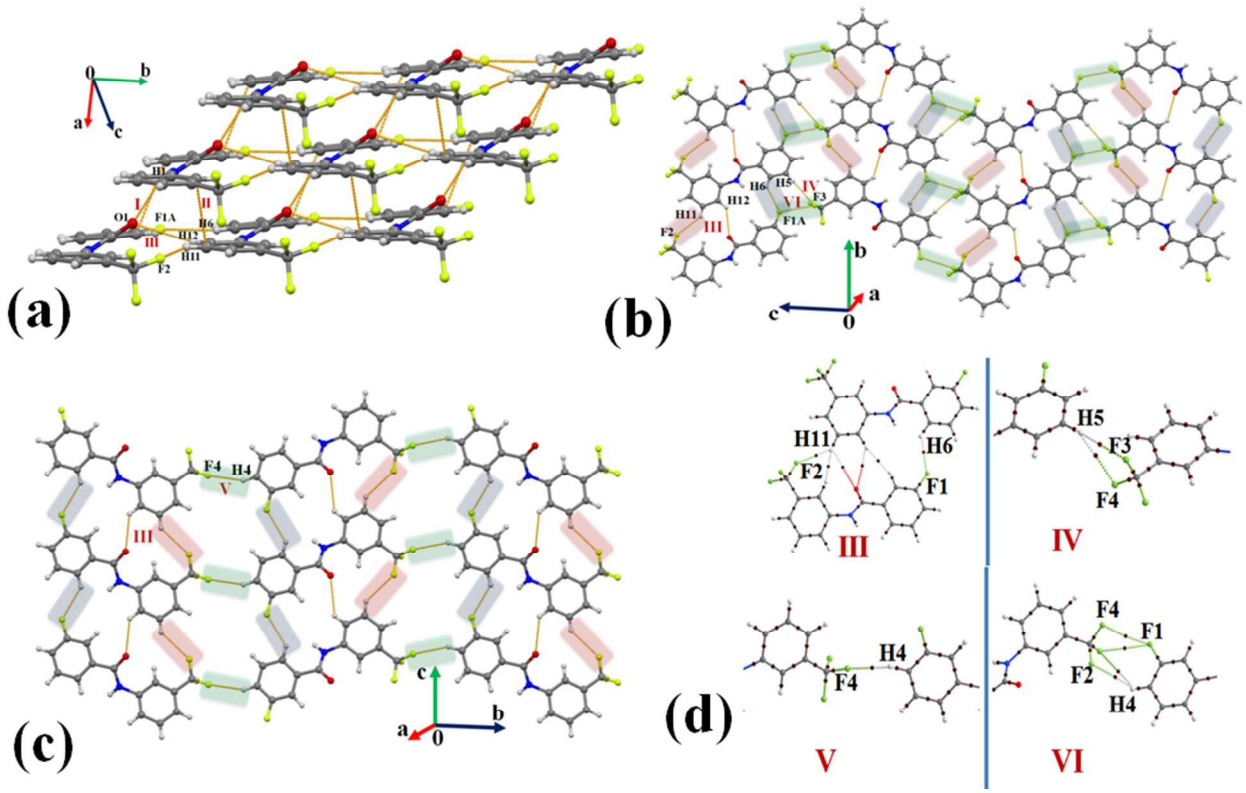

Figure 11(a): Packing of molecules in **2T2F** with the utilization of strong N-H···O=C, weak C-H···O, C-H···F-C_{sp2}, and C-H···F-C_{sp3} hydrogen bonds along with π···π interactions. **(b)** Formation of a molecular layer down the *bc* plane by the utilization of weak C-H···O, C-H··· F-C_{sp2}, and C-H···F-C_{sp3} hydrogen bonds and C_{sp3}-F···F-C_{sp3} interactions in **2T2F**. **(c)** Packing of molecules in **2T2F** *via* weak C-H···O=C, C-H···F-C_{sp2}, and C-H···F-C_{sp3} hydrogen bonds. **(d)** Selected molecular motifs (**Table S4**) in **2T2F**, showing different intermolecular interactions. Only interacting part of the motif was shown in case of **IV – VI**.

12) 4-fluoro-*N*-(2-(trifluoromethyl)phenyl)benzamide (1T3F):

The compound **1T3F** crystallizes in the centrosymmetric monoclinic space group $P2_1/n$ with two molecules in the asymmetric unit (Z = 8). The two most stabilized motifs **I** (-12.8 kcal/mol) and **II** (-12.7 kcal/mol), involving similar interactions (strong N-H···O=C hydrogen bond along with π···π interactions) were observe in the formation of a molecular chain of molecule **1** and **2** in the asymmetric unit respectively utilizing *n*-glide along *b*-axis [**Fig. 12(a)**]. Such chains are interconnected alternatively with the utilizations of motifs **III**, **IV**, **V** and **VII**. The motif **III** and **IV** provide similar stabilization (-4.4 kcal/mol and -4.1 kcal/mol respectively) and both are involved in the formation of highly short and directional C-H···O=C (2.29Å, 152°; 2.22Å, 167° respectively, **Table S3**) hydrogen bonds. A short C-H···F-C_{sp3} (2.56Å, 132°) along with a weak C-H···π hydrogen bond were noticed to connect the molecules in motif **V** whereas a near *type II* along with a near *type I* C_{sp3}-F···F-C_{sp2} interactions (2.983Å, 110°, 165°; 3.128Å, 90°, 117°) were recognized to stabilize (I.E being -2.7 kcal/mol) the crystal packing, existing as motif **VII** (**Table 2**). Further, packing of molecules in **1T3F** stabilized the formation of two dimeric motifs **VI** (-3.3 kcal/mol) and **VIII** (-2.1 kcal/mol) [**Fig. 12(b)**]. The motif **VI** involved two C-H···F-C_{sp3} hydrogen bonds along with weak C_{sp3}-F···F-C_{sp3} interactions (**Table S3**). And the dimeric motif **VIII** was observe to possess short C-H···F-C_{sp2} (2.48Å, 131°) hydrogen bond in the crystal packing in **1T3F**. Moreover, there were three equally stabilized (1.5 kcal/mol) molecular motifs **IX**, **X** and **XI** observed in the crystal packing and all were noticed to involve weak C-H···F-C hydrogen bonds (**Table 2**). Further a motif (**XII**, -1.3 kcal/mol), consisting of weak C_{sp2}-F···F-C_{sp2} interactions and connecting molecules '1' of the asymmetric unit, was observed to stabilize the crystal packing in **1T3F** [**Fig. 12 (c)**]. The weak C-H···F-C hydrogen bonds and C-F···F-C interactions, present in the motifs **V** to **XII** in **1T3F** were characterized by the theory of AIM. There were presence of (3, -1) BCPs observed for these interactions [**Fig. 12 (d)**].

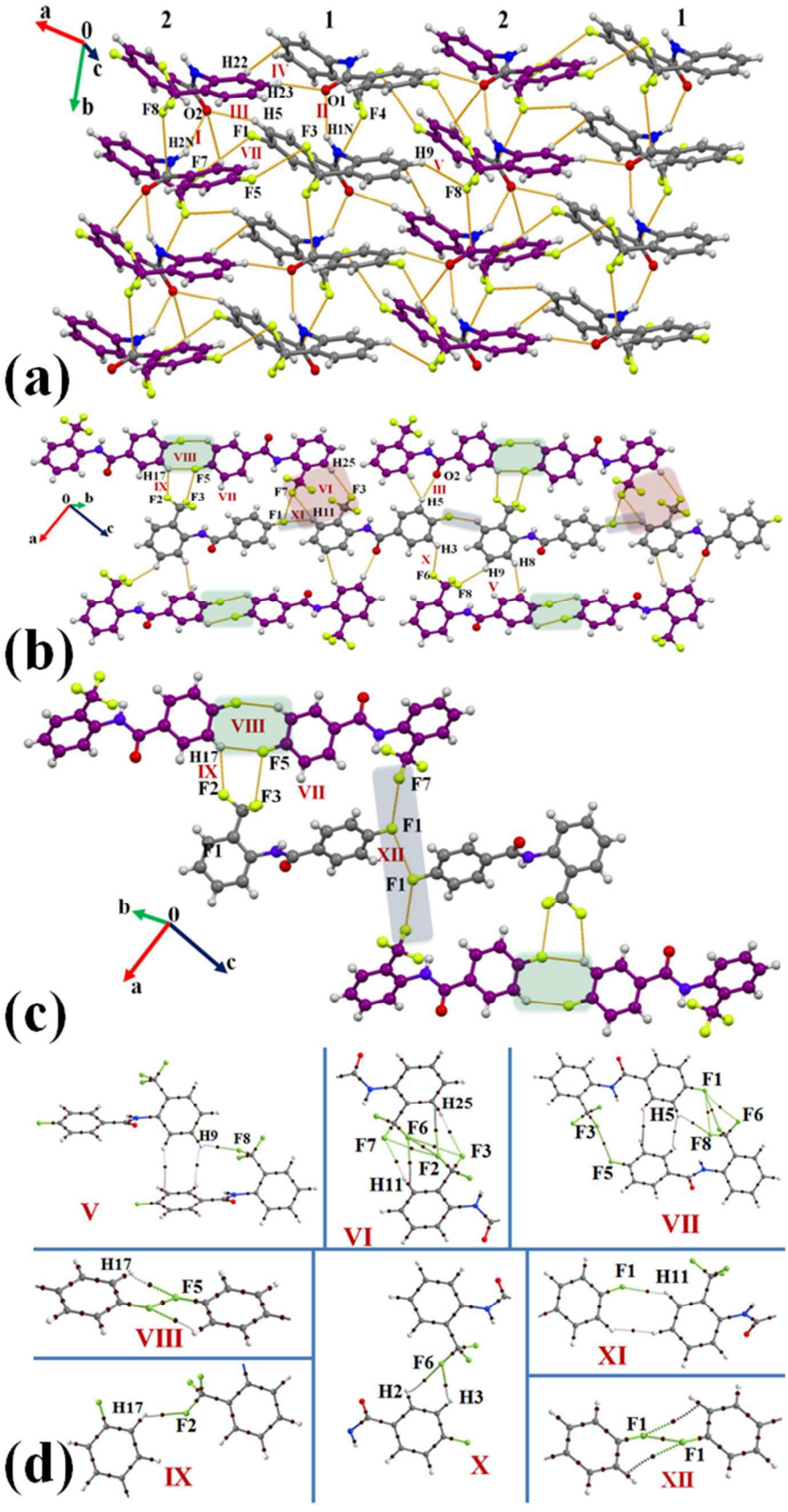

Figure 12(a) Packing of molecules in **1T4F** *via* the network of strong N-H···O=C, weak C-H···O, C-H···π, and C-H···F-$C_{sp3/sp2}$ hydrogen bonds along with C_{sp3}-F···C=O and C_{sp3}-F···F-C_{sp2} interactions. C-atoms in purple are shown for second molecule in the asymmetric unit. **(b)** Formation of molecular layer down the *ac* plane with the utilization of weak C-H···O=C, C-H···π, C-H···F-$C_{sp3/sp2}$ hydrogen bonds along with C_{sp3}-F···F-C_{sp2} interactions in **1T3F**. **(c)** Part of crystal packing in **1T3F**, showing the presence of weak C-H···F-$C_{sp3/sp2}$ hydrogen bonds along with C-F···F-C interactions. **(d)** Selected molecular motifs (**Table S4**) in **1T3F**, showing different intermolecular interactions. Only interacting part of the motif was shown in case of **V - XII**.

13) 4-fluoro-N-(4-(trifluoromethyl)phenyl)benzamide (3T3F):

The compound **3T3F** crystallizes in the centrosymmetric monoclinic space group $P2_1/c$ with Z = 4. A strong N-H···O=C hydrogen bond, supported by weak C-H···O=C and C-H···π hydrogen bond (motif **I**, 11.6 kcal/mol) was observed in the formation of a molecular chain utilizing c-glide perpendicular to *b*-axis in **3T3F** [**Fig. 13 (a)** & **13(b)**]. Such chains are interconnected *via* the motifs **II**, **III**, **V** and **VIII**. The weak π···π interactions were observed to connect molecules in the dimeric motifs **II** (-5.9 kcal/mol) and **III** (-4.6 kcal/mol). In the motif **V** (-2.6 kcal/mol), it was weak C-H···F-C_{sp2} hydrogen bond along with C-H···C=O interactions were recognized whereas a short C-H···F-C_{sp3}hydrogen bond was observed in motif **VIII** (-1.4 kcal/mol). The packing of the molecules in **3T3F** involved the formation of a herringbone pattern down the crystallographic *ab* plane with the utilization of motifs **IV** [-2.7 kcal/mol; involving short C-H···π hydrogen bond (2.79Å, 133°; **Table 2)**], **V** and **VIII** [**Fig. 13 (c)**]. Moreover, a bifurcated C-H···F-C_{sp2} hydrogen bond (motif **VII**, -2.2 kcal/mol), utilizing *c*-glide, was noticed in the formation of a molecular chain [**Fig. 13 (d)**].The chain was interlinked *via* the presence of motifs **VI**, **VIII** and **IX**. The motif **VI** (-2.6 kcal/mol) was found to involve the weak C-H···F-C_{sp3}hydrogen bond in the formation of a molecular chain utilizing *c*-glide [**Fig. 13 (d)**]. Dimeric and weakly stabilized (-0.4 kcal/mol) short C_{sp3}-F···F-C_{sp3} interactions were identified in the motif **IX**. The molecular motif **V- VIII** and **IX**, consisting of weak interactions involving fluorine, were studied topologically using the approach of QTAIM. Bond critical points at the bond path for these interactions were observed [**Fig. 13(e)**].

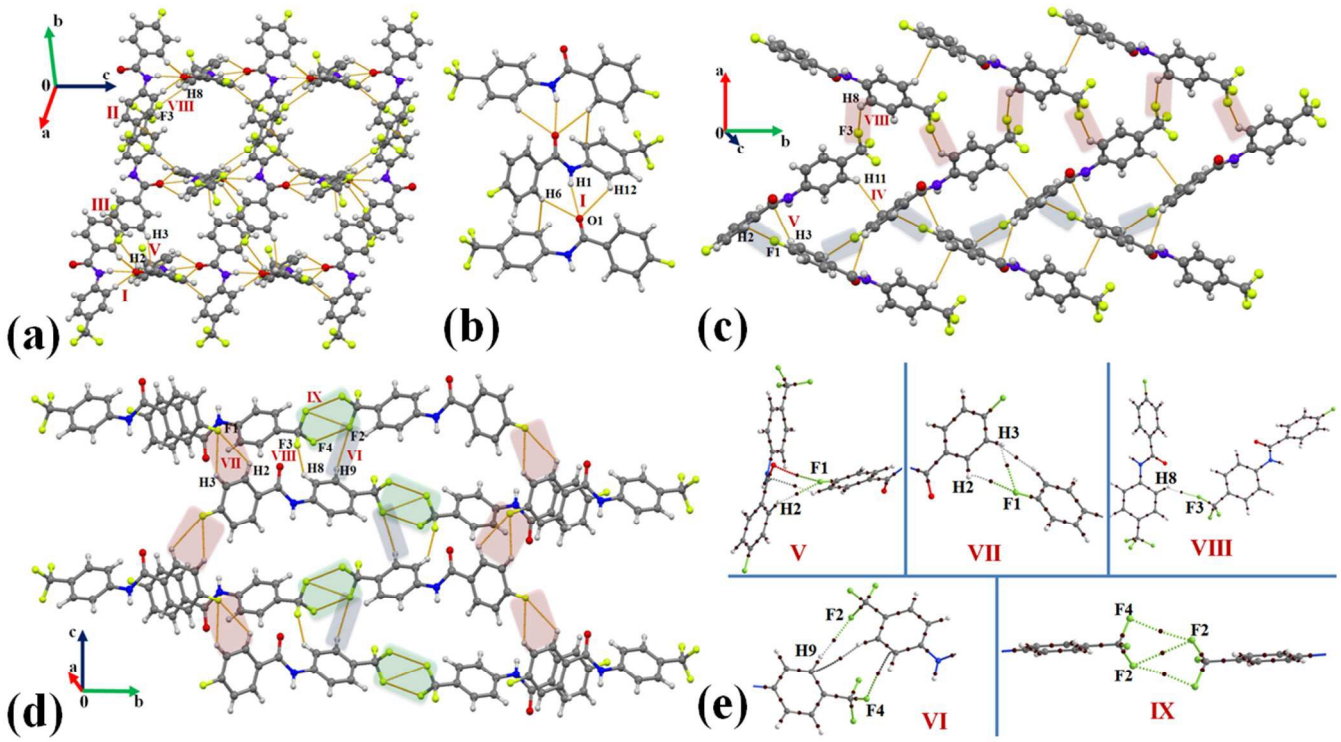

Figure 13 (a): Packing of molecules in **3T3F** *via* the network of strong N-H···O=C, weak C-H···O, C-H···π, C-H···F-C hydrogen bonds along with π···π interactions. **(b)** Depiction of a molecular chain *via* the motif **I** in **3T3F**. **(c)** Formation of a layer down the *ab* plane, utilizing weak C-H···F-C hydrogen bonds and C-H···C=O interactions in **3T3F**. **(d)** Formation of a weak bifurcated C-H···F-C hydrogen bonds along with C_{sp3}-F···F-C_{sp3} interactions down the *bc* plane in **3T3F**. **(e)** Selected molecular motifs (**Table S4**) in **3T3F**, showing different intermolecular interactions. Only interacting part of the motif was shown in case of **V - VII** and **IX**.

Therefore, the detailed analysis of all crystal structure revealed that the C(sp^2)/(sp^3)-F group were observed in the formation of different robust structural motifs in presence of a strong N-H···O=C hydrogen bond and other related weak interactions like C-H···O=C, C-H···π, and π···π. Moreover, in many cases, different supramolecular motifs (**Table S3**) by C(sp^2)/(sp^3)-F from the both side of the molecules can combine co-operatively in the formation of bigger structural motifs in the crystal structures.

Insights from Atoms in Molecules Calculations

It is of interest to do topological characterization of H···F and F···F interactions, observed in this class of compounds (including the previously reported crystal structures **[17, 38-40]**) and

analysis of the nature of these interactions along with the relationship of different topological parameters at BCP with bond path length. For this purpose, the selected dimers involving H···F or F···F interactions were identified and QTAIM calculations have been performed at their crystal geometry in accordance with the procedure reported in our earlier work **[40]**. The results of the calculations are presented in **Table S4** and **S5** of **Section S4** in ESI. Topological parameters for the selected C-H···F and C-F···F-C Interactions are given in **Table S4b**.

It is to be noted here that some of the important criteria for an interaction to be called a hydrogen bond or closed shell type are **[69 -70]**: (i) ρ value at BCP lies within the range [0.013, 0.270] e/Å^3 (ii) Positive value of the Laplacian of the electron density [$\nabla^2\rho > 0$)] indicates closed shell interactions (iii) The range of Laplacian values [$0.578 < \nabla^2\rho$ (e/Å^5) < 3.350] indicates the presence of a "*H-bond*" (iv) The value of $|V_b|/G_b < 1$ for hydrogen bond **[71 -72]** and closed shell interactions; V_b and G_b are the potential and kinetic energy density at BCP. It is of interest to validate the nature of H···F and F···F interactions with these criteria.

Analysis of H···F bonding interactions

H···F interactions were observed to lie in the range of 2.2Å – 3.0 Å for all structures in the current work. As observed earlier **[40]**, the dependent of electron density (ρ_b) shows exponential dependence with the bond path length (r_{ij}) [**Fig. 14(a)**] with the values in the range of $0.085 > \rho_b > 0.015$ e/Å^3. Hence these fulfill the criterion for the interactions to be called a hydrogen bond. The dissociation energy of these interactions (vary exponentially with r_{ij}, [**Fig. 14(b)**]) were observed between ~3.0 to ~0.4 kcal/mol. The value of Laplacian observed to be positive [$\nabla^2\rho >$ 0), **Fig. 14 (c)**] for the entire bond path length (r_{ij}) suggesting the closed shell nature of these H···F interactions. It is to be noted that for short C-H···F bond path length (r_{ij}) at less than the sum of van der Waal radii **[73]** of H and F, 2.67 Å, the values of the Laplacian are in accordance with the Koch and Popelier criteria for the existence of hydrogen bond [**74**]. Moreover, the values of $|V_b|/G_b$ were also observed to be less than one (criteria for hydrogen bond **[71 -72]**) for the entire range of bond path [**Fig. 14 (d)**].

Furthermore, it was of interest to study the role of hybridization of the C-atoms to which fluorine is attached in the C-H···F interactions. Hence the variation of dissociation energy (D.E) (kcal/mol) and electron density (e/Å^3) at BCP and with H···F bond path length (Å) for C-H···F-C(sp^2) and C-H···F-C(sp^3) have been compared [**Fig. 15(a)** & **15(b)**, **Table S4** and **S5**]. It was observed that the highest stabilized molecular motifs primarily consist of C(sp^2)-H···F-C(sp^2)

hydrogen bond in preference to C(sp^2)-H···F-C(sp^3) hydrogen bond in the crystal with the difference in energies of stabilization involving fluorine atoms attached to sp^2 and sp^3 carbon is not significant in molecular crystal [Circled area in **Fig 15(a) & (b)**].

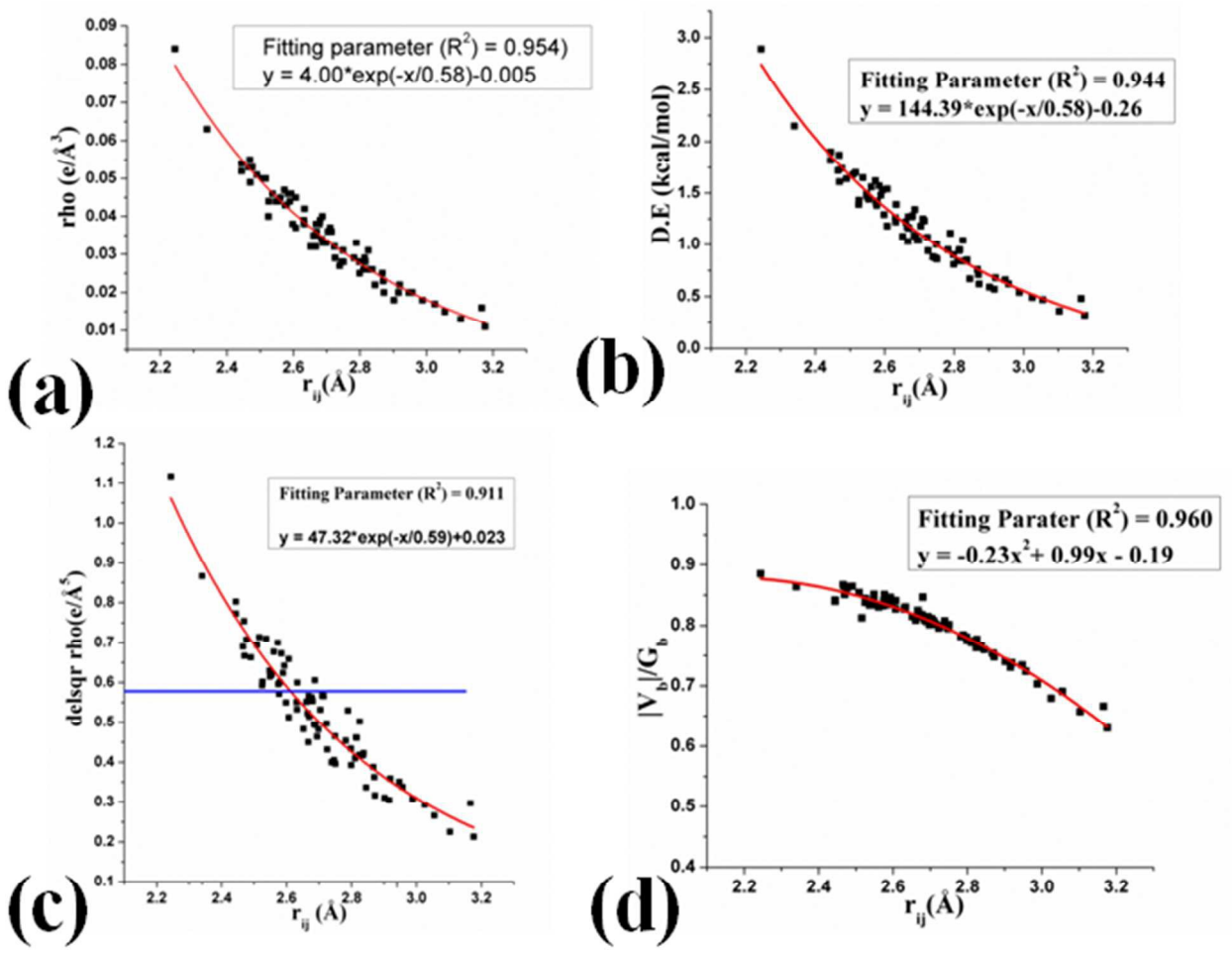

Figure 14: Variation of **(a)** electron density (e/Å^3) at BCP, **(b)** dissociation energy (D.E) (kcal/mol) with H···F bond path length (Å), **(c)** Laplacian ($\nabla^2\rho$) at BCP and **(d)** $|V_b|/G_b$ with H···F bond path length (Å).

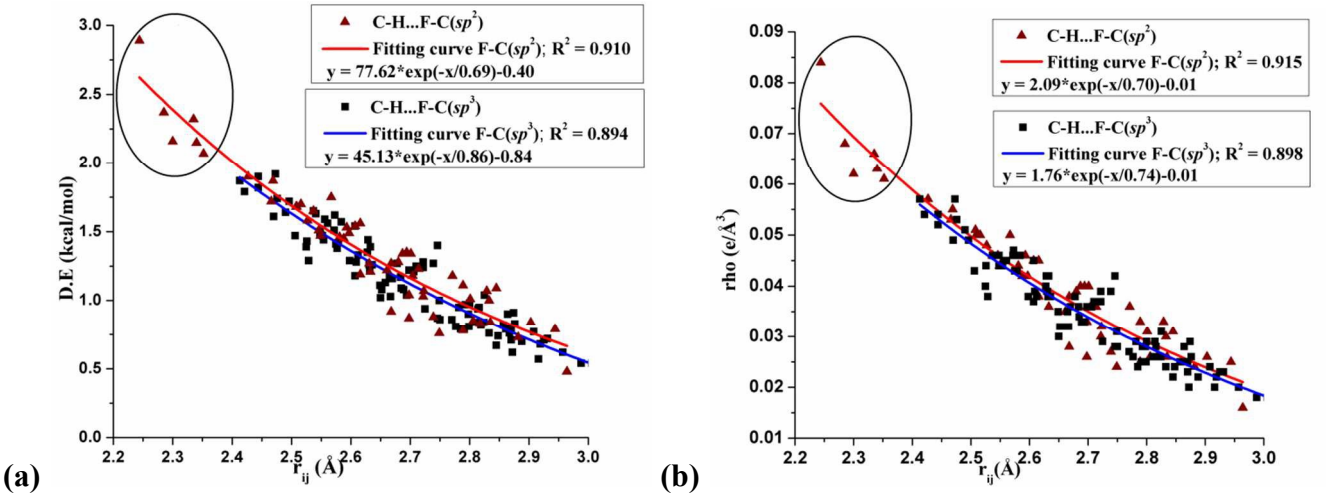

Figure 15: Comparison of variation of **(a)** dissociation energy (D.E) (kcal/mol) **(b)** electron density (e/Å^3) at BCP and with H···F bond path length (Å) for C-H···F-C(sp^2) [red curve] and C-H···F-C(sp^3) [blue curve] [Total 153 data points (98 for red curve and 55 for blue curve)].

Analysis of F···F bonding interactions

There are numerous C-F···F-C interactions observed in the crystal packing of this series of compounds (**Table S4** and **S5**). Hence, it was also of interest to do the topological characterization of F···F interactions. The nature and role of C-F···F-C interactions were recently studied both experimentally and theoretically by many researchers [**75 -76**]. The previous report by the QTAIM analysis of intramolecular C-F···F-C interactions on rigid isolated molecular system showed that these are closed shell interactions and can impart as much as 14 kcal/mol of local stabilization **[77]**. In the present work, QTAIM analysis of intermolecular C-F···F-C interactions has been performed and the result shows the exponential dependence of electron density at BCP (ρ_b), dissociation energy (D.E) and Laplacian ($\nabla^2\rho$) of the electron density at BCP with the F···F bond path length (r_{ij}) (**Fig. 16**). Values of electron density and dissociation energy (local stabilization) was observed between ~0.060 > ρ_b(e/Å^3) > ~0.010 and ~2.8 < D.E (kcal/mol) < ~0.5 for the ~2.80 > rij (Å) > 3.45. These values are slightly less or comparable with weak C-H···F-C interactions in the present work and observed to be similar to the previously observed values **[67, 77, 78 - 80]**. Furthermore, for the entire range of F···F bond path length, Laplacian ($\nabla^2\rho$) > 1 and $|V_b|/G_b$ < 1 were observed. Hence it can be concluded that the intermolecular F···F interactions in the present work are of closed shell in nature. Furthermore, the nature of C(sp^3)/(sp^2)-F···F-C(sp^3)/(sp^2) interactions from current and previous works along with reports

from experimental charge density analysis (**Table 1**) have been compared in **Figure 17**. The results shows the small differences in the in ρ_b(e/Å^3) at BCP for different type of C-F···F-C interactions involving fluorine atoms attached to an sp^2 and sp^3 carbon atom. The shorter C-F···F-C interactions were observed to be associated with the C(sp^2)-F bond in the molecule in the crystal. It is also of interest to notice variations in ρ_b, dissociation energy (D.E) and Laplacian ($\nabla^2\rho$) of the electron density at the BCP for a given value of r_{ij}. Different value of electron density at BCP for C(*sp*3)/(*sp*2)-F···F-C(*sp*3)/(*sp*2) interactions for the nearly same rij (A) of F···F bond path (near to sum of van der Waals radii of the F-atom, 2.94 A) in case of 3, 5, 6, 7, 8, 10 have been observed **[Fig. 18]**. This feature may be explained due to the cooperative interplay amongst the different possible intermolecular bond paths present in the motifs 3, 5, 6, 7 and 8 whereas in case of 10 (having the least value of ρb among these), only one C(*sp*3)-F···F-C(*sp*3) is present.

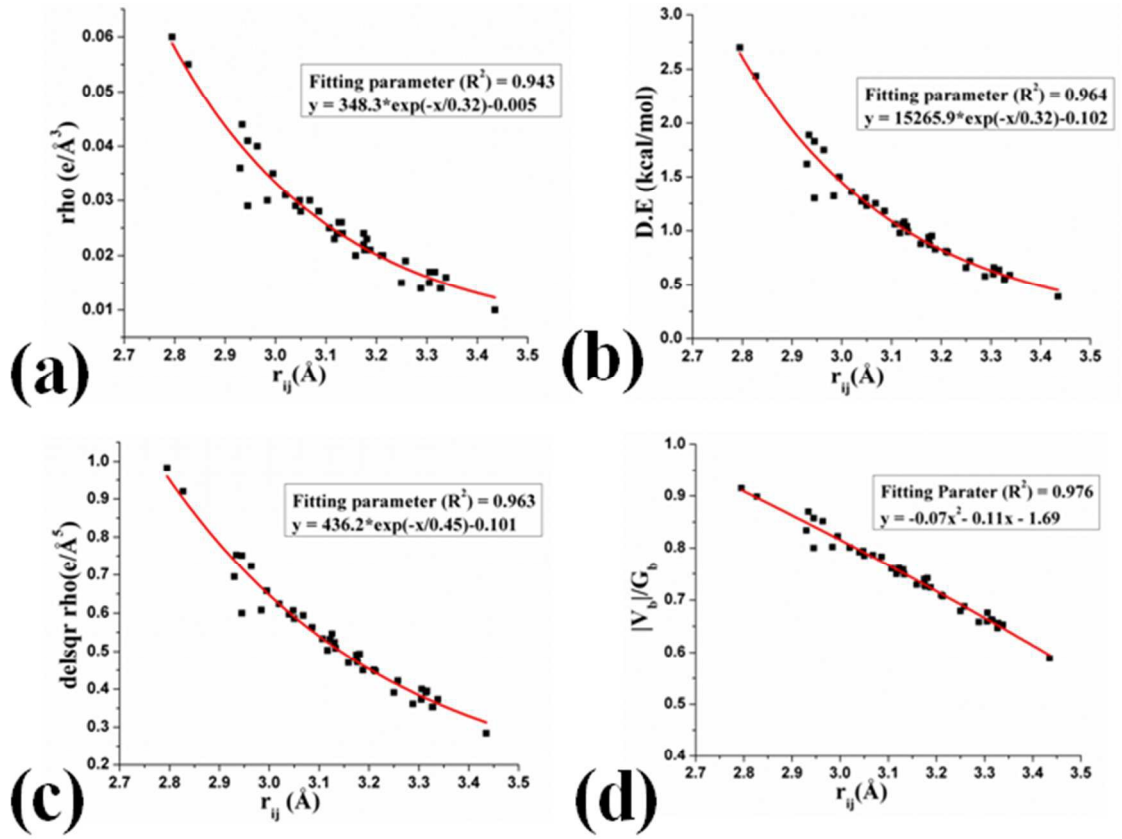

Figure 16: Variation of **(a)** electron density (e/Å^3), **(b)** dissociation energy (D.E) (kcal/mol) with F···F bond path length (Å) [42 data points], **(c)** Laplacian ($\nabla^2\rho$) at BCP and **(d)** $|V_b|/G_b$ with F···F bond path length (Å).

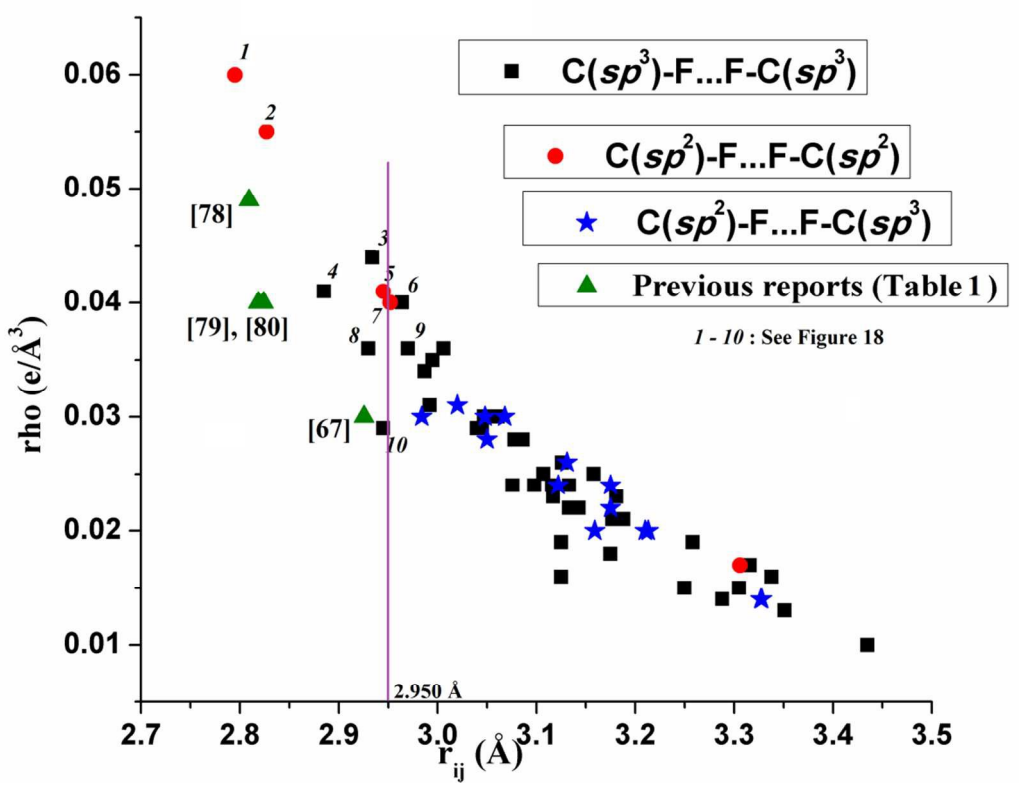

Figure 17: Comparison of the variation of the electron density (e/Å^3) at BCP and with F···F bond path length (Å) for C(sp^3)/(sp^2)-F···F-C(sp^3)/(sp^2) interactions from current and previous works [Total 64 data points].

Table 1: Topological parameters from previous reports on C-F···F-C interactions by charge density analysis of high resolution X-ray data.

Nature of Interactions	R_{ij} (Å)	ρ (e/Å^3)	$\nabla^2\rho$ (e/Å^5)	Reference
C(sp^2)-F···F-C(sp^2); *Type I*	2.8091	0.049	1.030	78
C(sp^2)-F···F-C(sp^2); *Type I*	2.8187	0.040	0.820	79
C(sp^2)-F···F-C(sp^2); *Type II*	2.8240	0.040	0.900	80
C(sp^3)-F···F-C(sp^3); *Type II*	2.9255	0.030	0.633	67

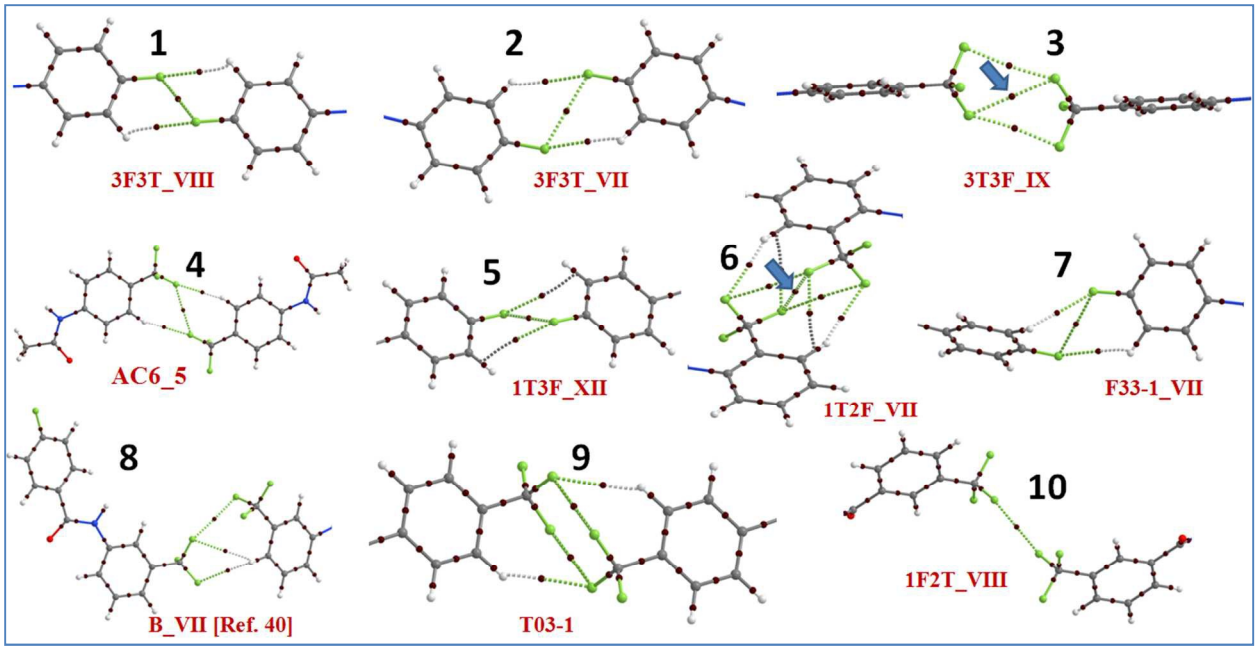

Figure 18: Showing first ten more stabilized motifs in **Fig. 17**, having C(sp^3)/(sp^2)-F···F-C(sp^3)/(sp^2) interactions near or below to sun of van der Waal radii of two F-atom, 2.94 Å.

Conclusion

Following the analysis of the 15 crystal structures (including one hydrate) from the 18 newly synthesized compounds along with the inputs from previously reported structures, the role of organic fluorine in the crystal packing have been analyzed in the presence of strong hydrogen bonds. Formation of many "reoccurring" structural motif by C_{sp2}-F and CF_3 group have been identified and investigated in terms of their nature, energetics and topological properties which were quantified by the PIXEL method and QTAIM approach. It was observed that the highest stabilized molecular motifs primarily consist of C(sp^2)-H···F-C(sp^2) hydrogen bond in preference to C(sp^2)-H···F-C(sp^3) H bond in the crystal. Moreover, formation of hydrogen bond by C(sp^2)/(sp^3)-F group were observed to be present over the entire distance range between 2.2 to 2.7Å (from the QTAIM approach), albeit the difference in energies of stabilization involving fluorine atoms attached to sp^2 and sp^3 carbon is not of significance in molecular crystals. Following the analysis of C(sp^2)/(sp^3)-F···F-C(sp^2)/(sp^3) interactions from QTAIM approach, it was observed that these fulfill the criteria of these being of the closed shell type for the entire F···F bond path length and provide *local* stabilization (indicates formation of bond) similar to the case of weak hydrogen bonds in crystals. For future study, it would be of interest to extend this

study to donor atoms in different hybridization environment with the F-C(sp^2)/(sp^3) group in different chemical environments. Furthermore, it is also of interest to investigate the effect of increasing fluorination on the molecule and the impact on the stabilization energies for the different supramolecular motifs involving organic fluorine present in the crystal.

Acknowledgements: PP thanks UGC-India for research scholarship. DC thanks IISER Bhopal for research facilities and infrastructure and DST-SERB for research funding.

References:

1. H.–J. Schneider, *Chem. Sci.*, 2012, **3**, 1381-1394.
2. G. K. S. Prakash, F. Wang, M. Rahm, J. Shen, C. Ni, R. Haiges and G. A. Olah, *Angew. Chem. Int. Ed*., 2011, **50**, 11761-1764.
3. F. F. Awwadi, R. D. Willett, K. A. Peterson and B. Twamley, *Chem. Eur. J*., 2006, **12**, 8952.
4. M. Perez-Torralba, M. A. Garcia, C. Lopez, M. C. Torralba, M. R. Torres, R. M. Claramunt and J. Elguer, *Cryst. Growth Des*., 2014, 14, 3499-3509.
5. I. Saraogi, V. G. Vijay, S. Das, K. Sekar and T. N. G. Row, *Cryst. Eng*., 2003, **6**, 69-77.
6. M. T. Scerba, S. Bloom, N. Haselton, M. Siegler, J. Jaffe and T. Lectka, *J. Org. Chem*., 2012, **77**, 1605-1609.
7. X. Xu, B. Pooi, H. Hirao and S. H. Hong, *Angew. Chem. Int. Ed*., 2014, **53**, 1283-1287.
8. R. Berger, G. Resnati, P. Metrangolo, E. Weber and J. Hulliger, *Chem. Soc. Rev*., 2011, **40**, 3496-3508 and references therein.
9. L. Shimoni and J. P. Glusker, *Struct. Chem*., 1994, **5**, 383-397.
10. J. A. K. Howard, V. J. Hoy, D. O'Hagan and G. T. Smith, *Tetrahedron*, 1996, **52**, 12613-12622.
11. J. D Dunitz and R. Taylor, *Chem. Eur. J.,* 1997, **3**, 89-98.
12. V. R. Thalladi, H.-C. Weiss, D. Blaser, R. Boese A. Nangia and G. R. Desiraju, *J. Am. Chem. Soc*., 1998, **120**, 8702-8710.
13. J. Parsch and J. W. Engels, *J. Am. Chem. Soc.,* 2002*,* **124***,* 5564-5572.
14. J. D. Dunitz, *Chem. Bio. Chem.,* 2004, **5**, 614-621.
15. J. D. Dunitz and W. B. Schweizer, *Chem. Eur. J.,* 2006, **12**, 6804-6815.

16. F. Cozzi, S. Bacchi, G. Filippini, T. Pilati and A. Gavezzotti, *Chem. Eur. J.,* 2007, **13**, 7177-7184.

17. D. Chopra and T. N. G. Row, *CrystEngComm*, 2008**, 10**, 54-67**.**

18. T. S. Thakur, M. T. Kirchner, D. Blaser, R. Boese and G. R. Desiraju, *CrystEngComm*, 2010, **12**, 2079-2085.

19. K. Muller, C. Faeh and F. Diederich, *Science*, 2007, **317**, 1881-1886.

20. D. Chopra and T. N. G. Row, *CrystEngComm*, 2011, **13**, 2175−2186 and references therein.

21. D. Chopra, *Cryst. Growth Des.,* 2012, **12***,* 541−546 and references therein.

22. P. A. Champagne, J. Desroches and J. –F. Paquin, *Synthesis,* 2015, **47**, 306-322 and references therein.

23. P. Panini and D. Chopra, In *Hydrogen Bonded Supramolecular Structures*, *Eds*. Z. Li and L. Wu, *Lecture Notes in Chemistry*, 2015, *Vol.* **87***,* pp. 37–67. Springer-Verlag, Berlin, Heidelberg. ISBN: 978-3-662-45755-9.

24. A. R. Choudhury and T. N. G. Row, *Cryst. Growth Des*., 2004, **4**, 47-52.

25. A. R. Choudhury and T. N. G. Row, *CrystEngComm*, 2006, **8**, 265-274.

26. D. Chopra, V. Thiruvenkatam, S. G. Manjunath and T. N. G. Row, *Cryst. Growth Des*., 2007, **7**, 868-874.

27. A. Schwarzer and E. Weber, *Cryst. Growth Des*., 2008, **8**, 2862-2874.

28. V. Vasylyeva and K. Merz, *Cryst. Growth Des*., 2010, **10**, 4250-4255.

29. V. Vasylyeva, O. V. Shishkin, A. V. Maleev and K. Merz, *Cryst. Growth Des*., 2012, **12**, 1032-1039.

30. M. Karanam and A. R. Choudhury, *Cryst. Growth Des*., 2012, **13**, 4803-4814.

31. G. Kaur, P. Panini, D. Chopra and A. R. Choudhury, *Cryst. Growth Des*., 2012, **12**, 5096-5110.

32. G. Kaur and A. R. Choudhury, *Cryst. Growth Des*., 2014, **14**, 1600 − 1616.

33. K. Merz, M. V. Evers, F. Uhl, R. I. Zubatyuk and O. V. Shishkin, *Cryst. Growth Des*., 2014, **14**, 3124-3130.

34. P. Panini and D. Chopra, *New J. Chem.,* 2015, **39**, 8720 — 8738.

35. A. Abad, C. Agullo, A. C. Cunat, C. Vilanova and M. C. R. de Arellano, *Cryst. Growth Des*., 2006, **6**, 46-57.

36. P. Mocilac, K. Donnelly and J. F. Gallagher, *Acta Crystallogr*., 2012, **B68**, 189-203.

37. R. Dubey, M. S. Pavan and G. R. Desiraju, *Chem Commun*., 2012, **48**, 9020-9022.

38. M. Perez-Torralba, M. A. Garcia, C. Lopez, M. C. Torralba, M. R. Torres, R. M. Claramunt and J. Elguer, *Cryst. Growth Des*., 2014, **14**, 3499-3509.

39. P. Panini and D. Chopra, *CrystEngComm*, 2013, **15**, 3711-3733.

40. P. Panini and D. Chopra, *CrystEngComm*, 2012, **14**, 1972-1989.

41. P. Panini and D.Chopra, *Cryst.Growth Des*., 2014, **14**, 3155-3168.

42. R. F. W. Bader, Atoms in Molecules: A Quantum Theory; Oxford University Press: Oxford, U.K., 1990.

43. (a) E. Arunan, G. R. Desiraju, R. A. Klein, J. Sadlej, S. Scheiner, I. Alkorta, D. C. Clary, R. H. Crabtree, J. J. Dannenberg, P. Hobza, H. G. Kjaeergaard, A. C. Legon, B. Mennucci and D. J. Nesbitt, *Pure. Appl. Chem*., 2011, **83**, 1619-1636. (b) E. Arunan, G. R. Desiraju, R. A. Klein, J. Sadlej, S. Scheiner, I. Alkorta, D. C. Clary, R. H. Crabtree, J. J. Dannenberg, P. Hobza, H. G. Kjaeergaard, A. C. Legon, B. Mennucci and D. J. Nesbitt, *Pure. Appl. Chem*., 2011, **83**, 1637-1641.

44. A. Gavezzotti, A. *New. J. Chem*., 2011, **35**, 1360 − 1368.

45. A. Gavezzotti, Mol. Phys. 2008, **106**, 1473 – 1485.

46. L. Maschio, B. Civalleri, P. Ugliengo and A. Gavezzotti, *J. Phys. Chem. A*, 2011, **115**, 11179-11186.

47. J. D. Dunitz and A. Gavezzotti, *Cryst. Growth Des*., 2012, **12**, 5873-5877.

48. R. Shukla and D. Chopra, *CrystEngComm*, 2015, **17**, 3596-3609.

49. V. Petricek, M. Dusek and L. Palatinus, *JANA 2000*, 18/12/2007; Institute of Physics, Czech Republic, 2007; http://jana.fzu.cz.

50. A. Altomare, G. Cascarano, C. Giacovazzo and A. Guagliardi, *J. Appl. Crystallogr*., 1993, **26**, 343-350.

51. G. M. Sheldrick, *Acta Crystallogr*., 2008, **A64**, 112-122.

52. L. J. Farrugia, *WinGX, J. Appl. Crystallogr*., 1999, **32**, 837-838.

53. C. F. Macrae, I. J. Bruno, J. A. Chisholm, P. R. Edgington, P. McCabe, E. Pidcock, L. Rodriguez-Monge, R. Taylor, J. Streek and P. A. Wood, *J. Appl. Crystallogr*., 2008, **41**, 466-470, www.ccdc.cam.ac.uk/mercury.

54. P. Panini, K. N. Venugopala, B. Odhav and D. Chopra, *Acta Cryst*., 2014, **B70**, 681-696.

55. R. Shukla, T. P. Mohan, B. Vishalakshi and D. Chopra, *CrystEngComm*, 2014, **16**, 1702-1713.

56. D. Dey, T. P. Mohan, B. Vishalakshi and D. Chopra, D. *Cryst. Growth Des*., 2014, **14**, 5881-5896.

57. P. Panini, R. Shukla, T. P. Mohan, B. Vishalakshi and D. Chopra, *J. Chem. Sci*., 2014, **126**, 1337-1345.

58. S. Grimme, J. Antony, S. Ehrlich and H. Krieg, *J. Chem. Phys*., 2010, **132**, 154104-154119.

59. W. Hujo and S. Grimme, *Phys. Chem. Chem. Phys*., 2011, **13**, 13942-13950.

60. R. Ahlrichs, M. Baer, M. Haeser, H. Horn and C. Koelmel, Elec*tr*onic structure calculations on work- station computers: the program system TURBOMOLE. *Chem. Phys. Lett*., 1989, **162**, 165-169.

61. F. Bernardi and S. F. Boys, *Mol. Phys*., 1970, **19**, 553.

62. T. A. Keith, *AIMALL, version 13.05.06*; TK Gristmill Software, Overland Park KS, USA, **2013**; aim.tkgristmill.com.

63. E. Espinosa, E. Molins and C. Lecomte, *Chem. Phys. Lett*., 1998, **285**, 170-173.

64. I. Mata, I. Alkorta, E. Espinosa and E. Molins, *Chem. Phys.Lett.,* 2011, **507**, 185-189.

65. M. V. Vener, A. N. Egorova, A. V. Churakov and V. G. Tsirelson, *J. Comput. Chem*., 2012, **33**, 2303-2309.

66. E. D'Oria and J. J. Novoa, *CrystEngComm*., 2008, **10**, 423-436.

67. V. R. Hathwar, D. Chopra, P. Panini and T. N. G. Row, *Cryst. Growth. Des*., 2014, **14**, 5366-5369.

68. R. M. Osuna, V. Hernåndez, J. T. L. Navarrete, E. D'Oria and J. J. Novoa, *Theor Chem Acc*., 2011, **128**, 541-553.

69. P. L. Popelier, *Atoms in Molecules: An Introduction*; Prentice Hall: London, **2000**.

70. U. Koch and P. L. A. Popelier, *J. Phys. Chem*., 1995, **99**, 9747-9754.

71. I. Mata, I. Alkorta, E. Molins and E. Espinosa, *Chem.-Eur. J*., 2010, **16**, 2442-2452.

72. E. Espinosa, I. Alkorta, J. Elguero and E. Molins, *J. Chem. Phys*., 2002, **117**, 5529-5542.

73. A. Bondi, *J. Phys. Chem*., 1964, **68**, 441-451.

74. G. Zhang, W. He, D. Chen, *Mol. Phys*., 2014, **112**, 1736-1744.

75. R. J. Baker, P. E. Colavita, D. M. Murphy, J. A. Platts and J. D. Wallis, *J. Phys. Chem. A* 2012, **116**, 1435-1444.

76. R. A. Cormanich, R. Rittner, D. O'Hagan and M. Bühl, *J. Phys. Chem. A*, 2014, **118**, 7901-7910.

77. C. F. Matta, N. Castillo and R. J. Boyd, *J. Phys. Chem. A*, 2005, **109**, 3669-3681.

78. D. Chopra, T. S. Cameron, J. D. Ferrara and T. N. G. Row, *J. Phys. Chem. A*, 2006, **110**, 10465-10477.

79. V. R. Hathwar and T. N. G. Row, *Cryst. Growth Des.* 2011, **11**, 1338-1346.

80. M. S. Pavan, K. D. Prasad and T. N. G. Row, *Chem. Commun*., 2013, **49**, 7558−7560.

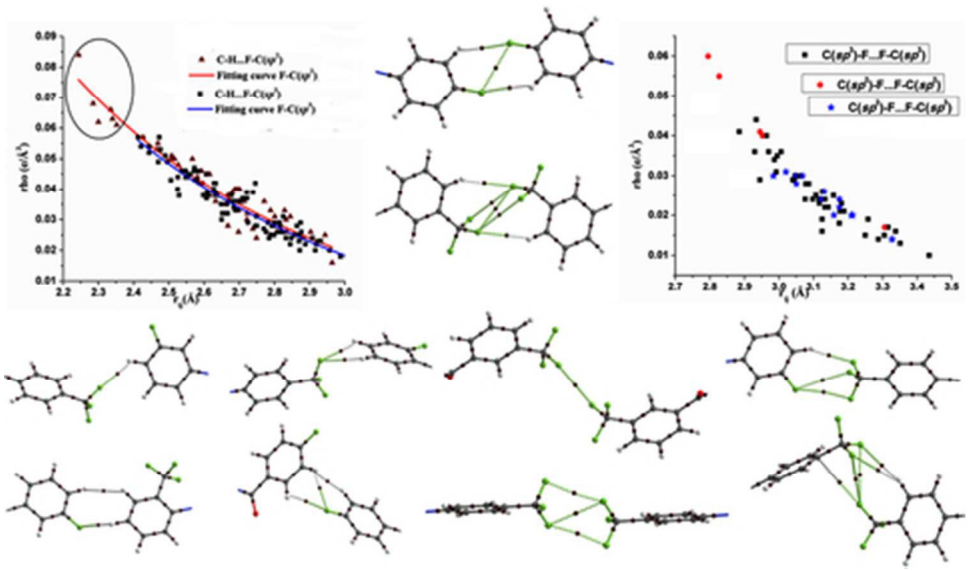

40x23mm (300 x 300 DPI)